
IGLU: Efficient GCN Training via Lazy Updates

S Deepak Narayanan* ^{||}
 Microsoft Research, India
 Bengaluru, 560001
 sdeepaknarayanan1@gmail.com

Aditya Sinha* [‡]
 Microsoft Research, India
 Bengaluru, 560001
 adityaasinha28@gmail.com

Prateek Jain* [‡]
 Microsoft Research, India
 Bengaluru, 560001
 pjain9@gmail.com

Purushottam Kar†
 IIT Kanpur & Microsoft Research, India
 purushot@cse.iitk.ac.in

Sundararajan Sellamanickam
 Microsoft Research, India
 Bengaluru, 560001
 ssrajan@microsoft.com

Abstract

Graph Convolution Networks (GCN) are used in numerous settings involving a large underlying graph as well as several layers. Standard SGD-based training scales poorly here since each descent step ends up updating node embeddings for a large portion of the graph. Recent methods attempt to remedy this by sub-sampling the graph which does reduce the compute load, but at the cost of biased gradients which may offer suboptimal performance. In this work we introduce a new method IGLU that caches forward-pass embeddings for all nodes at various GCN layers. This enables IGLU to perform lazy updates that do not require updating a large number of node embeddings during descent which offers much faster convergence but does not significantly bias the gradients. Under standard assumptions such as objective smoothness, IGLU provably converges to a first-order saddle point. We validate IGLU extensively on a variety of benchmarks, where it offers up to 1.2% better accuracy despite requiring up to 88% less wall-clock time.

1 Introduction

The Graph Convolution Network (GCN) model has received much attention as an effective graph representation learning technique. It can exploit network topology while embedding data points enabling superior performance in several applications including immediate ones such as node classification on graphs [13] and recommendation systems [18] but also innovative ones such as program repair [17].

Their success notwithstanding, training GCNs at scale remains a challenging task especially on large and dense graphs with architectures involving multiple convolutional layers. The main reason behind this is the aggregation operation that enables GCNs to adapt to graph topology, in the first place. A node's output layer embedding in a GCN is influenced by embeddings of its neighbors in the previous layer which recursively depend on embeddings of their own neighbors in the still previous layer, and so on. Even in GCNs with 2-3 layers, this causes back propagation initiated at a particular node to end up directing updates at a large multi-hop neighborhood, especially in dense graphs.

* denotes equal contribution. [†]Work done at Microsoft Research, India. [‡]Now at Google Research, India.
^{||}Now at ETH Zurich.

Unfortunately, this causes mini-batch SGD-based techniques to scale poorly since a large fraction of the graph needs to be processed in every iteration even though loss terms for only a few nodes may be getting considered in any mini-batch. Most of the effort invested in overcoming this problem focuses on sampling- or clustering-based techniques that contain this neighborhood *explosion* by limiting the number of nodes that receive updates as a result of a back-propagation step [5, 8, 20]. As sampling introduces additional variance into training, variance reduction techniques have also been studied [3]. However, several of these techniques require the graph to be heavily subsampled to scale to large graphs which results in poor accuracy due to insufficient aggregation. These techniques also seldom guarantee unbiased gradients and do not offer rigorous convergence guarantees. See Section 2 for a more detailed discussion about state-of-the-art methods for GCN training.

Our Contributions: This paper presents IGLU, an efficient technique for training GCNs based on lazy updates. An analysis of the gradient structure in GCNs reveals that the most expensive component of the back-propagation step initiated at a node is in fact (re-)computing forward-pass embeddings for its vast multi-hop neighborhood. Based on this observation, IGLU caches node embeddings at regular intervals. These stale embeddings can be used to perform back-propagation with significantly reduced complexity. This presents a stark departure from the current state-of-the-art in completely avoiding sampling steps. The resulting technique is architecture-agnostic and can be implemented on a wide range of GCN architectures with little effort. Avoiding sampling also allows IGLU to completely avoid the associated variance artifacts and offer provable convergence to a first-order stationary point under standard assumptions. In experiments, IGLU was found to offer superior accuracies or accelerated convergence on a range of benchmark datasets.

2 Related Works

The works of [2, 7, 13] established GCN as an attractive architecture for transductive learning tasks on graphs. Subsequent works expanded the scope of GCNs to inductive settings as well as explored architectural variants such as the GIN [16]. A substantial amount of effort, mostly focused on sampling strategies, has gone into speeding up GCN training.

The simplest of these strategies is the *neighborhood sampling* strategy adopted by GraphSAGE [8] which iteratively sub-samples the multi-hop neighborhood of a node before proceeding to initiate back-propagation at that node. Only the sub-sampled neighbors participate in the back-propagation step that limits the amount of computation required. *Layer sampling* strategies further decreased the computation requirement and has been adopted by FastGCN [4], LADIES [21] and ASGCN [11]. These methods sample a subset of nodes for each layer in the GCN, often using importance sampling to reduce variance and improve connectivity among the sampled nodes. FastGCN used the same sampling distribution for all layers and could struggle to maintain connectivity unless large batch-sizes were used. In contrast, LADIES used a per-layer distribution with the distribution for a layer conditioned on nodes that were sampled for the layer above which allowed for more efficient use of samples when operating on a budget. ASGCN used a linear model to jointly infer node importance weights to construct the sampling distribution. More recent works such as Cluster-GCN [5] and GraphSAINT [20] have proposed *subgraph sampling* which create mini-batches out of subgraphs. Backpropagation updates are then restricted to nodes within the chosen subgraph. To avoid losing too many edges, mini-batch sizes need to be enlarged. To this end, Cluster-GCN identifies its subgraphs via graph clustering and chooses multiple clusters per mini-batch while reinserting cross-cluster edges whereas GraphSAINT samples large subgraphs directly using random walks.

Bias and Variance: Sampling techniques face not only sampling variance but also bias as navigating the myriad non-linearities in the GCN architecture make it difficult to construct unbiased estimates. For instance, [20] show certain un-biasedness properties if non-linearities are discarded. Nevertheless, several variance-reduction techniques have been proposed to tackle variance due to sampling as well as mini-batch creation. Examples include VR-GCN [3], MVS-GNN [6] and AS-GCN [11]. VR-GCN samples nodes uniformly at each layer whose embeddings are to be updated and uses stale embeddings for rest of the nodes. Under suitable conditions, VRGCN assures variance elimination in the limit. MVS-GNN augments this to reduce variance due to mini-batch creation by performing importance weighted sampling based on gradient norms of the nodes to construct mini-batches.

IGLU in Context of Related Work: IGLU completely avoids sampling as a strategy and instead performs speedy updates using stale node embeddings that are cached and lazily updated at regular

intervals. Computing these embeddings in bulk offers IGLU economies of scale. Moreover, the method faces zero sampling variance but does incur a bias due to using stale embeddings. Fortunately, this bias can be shown to be not just bounded, but can also be made arbitrarily small by adjusting the step length and frequency of refreshing the node embeddings.

3 IGLU: Efficient GCN Training via Lazy Updates

Problem Statement: We consider the problem of learning a GCN architecture on an undirected graph $\mathcal{G}(\mathcal{V}, \mathcal{E})$ with each of the N nodes in the graph endowed with an *initial* feature vector $\mathbf{x}_i^0 \in \mathbb{R}^{d_0}, i \in \mathcal{V}$. Let $X^0 \in \mathbb{R}^{n \times d_0}$ denote the matrix of these initial features stacked together. The set of neighbors of a node i to which it has edges is denoted by $\mathcal{N}(i) \subset \mathcal{V}$. Let A denote the (normalized) adjacency matrix of this graph. A multi-layer GCN architecture adopts a parameterized function for each of its layers to aggregate information from a node’s own embedding as well as those of its neighbors to obtain that node’s embedding for the next layer. Specifically,

$$\mathbf{x}_i^k = f(\mathbf{x}_i^{k-1}, j \in \{i\} \cup \mathcal{N}(i); E^k),$$

where E^k denotes the parameters of k -th layer. For example, a standard GCN layer is given by,

$$\mathbf{x}_i^k = \sigma \left(\sum_{j \in \mathcal{V}} A_{ij} (W^k)^\top \mathbf{x}_j^{k-1} \right),$$

where E^k is simply the matrix $W^k \in \mathbb{R}^{d_{k-1} \times d_k}$ where d_k is the embedding dimensionality after the k^{th} layer. However, more involved architectures exist that incorporate operations such as layer normalization, batch normalization. In this paper, we will continue to use E^k to denote the collection of all parameters of the k^{th} layer, for instance offset and scale parameters used in a layer norm operation. Let $X^k \in \mathbb{R}^{n \times d_k}$ denote the matrix of k^{th} layer embeddings stacked together. This gives us the handy shorthand $X^k = f(X^{k-1}; E^k)$. Given a K -layer GCN and a multi-label/multi-class task with C labels/classes, a fully-connected layer $W^{K+1} \in \mathbb{R}^{d_K \times C}$ and appropriate activation function such as softmax is applied to get predictions which are then fed into the task loss. We note that IGLU does not require the task loss to decompose over the classes. The convergence proofs simply require that the training objective function is smooth.

Neighborhood Explosion: To analyze the core reason behind neighborhood explosion and hence expensive standard GCN training, we consider a univariate regression problem with a no-frills 2-layer GCN endowed with unidimensional features and sigmoidal activation within the hidden layers i.e. $K = 2$ and $C = 1 = d_0 = \dots = d_k$. This GCN is parameterized by $w^1, w^2, w^3 \in \mathbb{R}$ and offers the output $\hat{y}_i = w^3 \sigma(z_i^2)$ where $z_i^2 = \sum_{j \in \mathcal{V}} A_{ij} w^2 x_j^1 \in \mathbb{R}$. In turn, we have $x_j^1 = \sigma(z_j^1)$ where $z_j^1 = \sum_{j' \in \mathcal{V}} A_{jj'} w^1 x_{j'}^0 \in \mathbb{R}$ and $x_{j'}^0 \in \mathbb{R}$ are the initial features of the nodes. Given a task loss $\ell : \mathbb{R}^N \times \mathbb{R}^N$ e.g. least squares, denoting $\ell'_i = \ell'(\hat{y}_i, y_i)$ gives us

$$\begin{aligned} \frac{\partial \ell(\hat{y}_i, y_i)}{\partial w^1} &= \ell'_i \cdot \frac{\partial \hat{y}_i}{\partial z_i^2} \cdot \frac{\partial z_i^2}{\partial w^1} = \ell'_i \cdot w^3 \sigma'(z_i^2) \cdot \sum_{j \in \mathcal{V}} A_{ij} w^2 \frac{\partial x_j^1}{\partial w^1} \\ &= \ell'_i \cdot w^3 \sigma'(z_i^2) \cdot \sum_{j \in \mathcal{V}} A_{ij} w^2 \sigma'(z_j^1) \cdot \sum_{j' \in \mathcal{V}} A_{jj'} x_{j'}^0. \end{aligned}$$

The nesting of the summations is conspicuous and establishes the neighborhood explosion: when seeking gradients in a K -layer GCN on a graph with average degree m , upto an m^{K-1} -sized neighborhood of a node may be involved in the back-propagation update initiated at that node. Note also that the above expression involves terms such as $\sigma'(z_i^2), \sigma'(z_j^1)$ and that the values of z_i^2, z_j^1 etc change whenever the model receives updates. Consequently, for a fresh mini-batch of nodes chosen for a particular iteration, terms such as $\sigma'(z_i^2), \sigma'(z_j^1)$ need to be computed afresh if the gradient is to be computed exactly. Performing these computations amounts to doing *forward pass operations* that frequently involve a large neighborhood of the nodes in a chosen mini-batch. Sampling strategies try to limit this cost by directly restricting the neighborhood over which such forward passes are needed. However, this introduces both bias and variance into the gradient updates as discussed in Section 2. As described below, IGLU identifies this limitation and chooses to lazily update various *incomplete gradient* (defined below) and node embedding terms that participate in the above expression. These

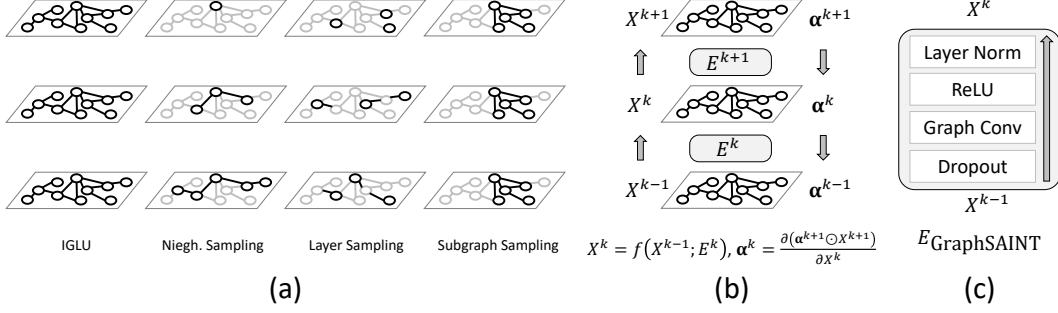


Figure 1: Fig 1(a) highlights the distinction between existing sampling-based approaches which introduce bias and variance in training due to the sampling operations, and IGLU which completely sidesteps these issues, instead being able to scalably execute GCN back-propagation steps on the full graph owing to its use of lazy updates which offer no sampling variance and provably bounded bias. Fig 1(b) summarizes the quantities useful in IGLU's updates. IGLU is architecture-agnostic and can be readily used with wide range of existing architectures. Fig 1(c) gives an example of a GCN layer architecture used by the GraphSAINT method.

completely eliminate sampling variance but introduce a bias due to the use of stale terms. However, the following discussion shows how this bias is not just bounded, but can also be made arbitrarily small by adjusting the step length and frequency of refreshing these stale incomplete gradient and node embedding terms.

Lazy Updates for GCN Training: Consider an arbitrary GCN architecture with the following structure: for some parameterized layer functions we have $X^k = f(X^{k-1}; E^k)$ where E^k denotes the collection of all parameters of the k^{th} layer, for instance weight matrices or offset and scale parameters used in layer norm operations. $X^k \in \mathbb{R}^{n \times d_k}$ denotes the matrix of k^{th} layer embeddings stacked together and X^0 are the initial features. For a K -layer GCN on a multi-label/multi-class task with C labels/classes, a fully-connected layer $W^{K+1} \in \mathbb{R}^{d_K \times C}$ is additionally included to offer $\hat{y}_i = (W^{K+1})^\top x_i^K \in \mathbb{R}^C$. Let us use the shorthand $\hat{Y} \in \mathbb{R}^{N \times C}$ to denote the matrix where the predicted outputs \hat{y}_i over all the nodes are stacked. We assume a task loss function $\ell : \mathbb{R}^C \times \mathbb{R}^C \times \mathbb{R}_+$ that need not decompose over the classes. We will use the abbreviation $\ell_i := \ell(\hat{y}_i, y_i)$. For sake of simplicity, we assume that the loss function itself includes any activation such as softmax that needs to be applied over the predictions \hat{y}_i . Let $\mathcal{L} = \sum_{i \in \mathcal{V}} \ell_i$ denote the total loss function.

We define the the *loss derivative* matrix $\mathbf{G} = [g_{ic}] = \mathbb{R}^{N \times C}$ as $g_{ic} := \frac{\partial \ell_i}{\partial \hat{y}_{ic}}$ where we recall that $\hat{y}_i = [\hat{y}_{ic}] \in \mathbb{R}^C$ are the outputs of the network that are fed into the loss function. Note that this definition is sound even for loss functions that do not decompose over the classes. We also introduce the following *incomplete gradient* terms. These capture the dependence of the task loss on intermediate layer node embeddings offered by the GCN and are critical to the functioning of IGLU.

Definition 1. For the notation described above, for any layer $k \leq K$, define its *incomplete task gradient* to be $\alpha^k = [\alpha_{jp}^k] \in \mathbb{R}^{N \times d_k}$, where,

$$\alpha_{jp}^k := \left. \frac{\partial (\mathbf{G} \odot \hat{Y})}{\partial X_{jp}^k} \right|_{\mathbf{G}} = \sum_{i \in \mathcal{V}} \sum_{c \in [C]} g_{ic} \cdot \frac{\partial \hat{y}_{ic}}{\partial X_{jp}^k}.$$

The following lemma completely characterizes the gradients of the various parameters in the GCN in terms of the loss derivative matrix \mathbf{G} and the incomplete gradient terms $\alpha^k, k \in [K]$, as well as give recursive closed-form expressions to calculate the incomplete gradient terms for any layer.

Lemma 1. The following results hold whenever the task loss \mathcal{L} is differentiable:

1. For the final fully-connected layer we have $\frac{\partial \mathcal{L}}{\partial W^{K+1}} = (X^K)^\top \mathbf{G}$ as well as for any $k \in [K]$ and any parameter E^k in the k^{th} layer, $\frac{\partial \mathcal{L}}{\partial E^k} = \left. \frac{\partial (\alpha^k \odot X^k)}{\partial E^k} \right|_{\alpha^k} = \sum_{i \in \mathcal{V}} \sum_{p=1}^{d_k} \alpha_{ip}^k \cdot \frac{\partial X_{ip}^k}{\partial E^k}$.
2. For the final layer, we have $\alpha^K = \mathbf{G} (W^{K+1})^\top$ as well as for any $k < K$, we have $\alpha^k = \left. \frac{\partial (\alpha^{k+1} \odot X^{k+1})}{\partial X^k} \right|_{\alpha^{k+1}}$ i.e. $\alpha_{jp}^k = \sum_{i \in \mathcal{V}} \sum_{q=1}^{d_{k+1}} \alpha_{iq}^{k+1} \cdot \frac{\partial X_{iq}^{k+1}}{\partial X_{jp}^k}$.

It is important to note that Lemma 1 establishes a recursive definition of the incomplete derivatives using terms such as $\frac{\partial X_{iq}^{k+1}}{\partial X_{jp}^k}$ that only concern a single layer. Thus, computing α^k for any $k \in [K]$ does not involve any neighborhood explosion since only the immediate neighbors of a node need be consulted. Moreover, Lemma 1 also shows that if α^k are computed and frozen, the model derivatives $\frac{\partial \mathcal{L}}{\partial E^k}$ only involve additional computation of terms such as $\frac{\partial X_{ip}^k}{\partial E^k}$ which yet again involve a single layer and do not cause neighborhood explosion. This motivates lazy updates to α^k , X^k values in order to accelerate back-propagation. However, as we shall see later, performing lazy updates to both α^k , X^k offers suboptimal performance. Hence IGLU adopts two variants described in Algorithms 1 and 2. The *backprop* variant* keeps embeddings X^k stale for an entire epoch but performs eager updates to α^k . The *inverted* variant on the other hand keeps the incomplete gradients α^k stale for an entire epoch but performs eager updates to X^k . We note that update steps in the algorithms (steps 4, 8 in Algorithm 1 and steps 7, 10 in Algorithm 2) are described as a single gradient step over the entire graph to simplify exposition – in practice these steps are implemented using *mini-batch* SGD.

Algorithm 1 IGLU: backprop order

Input: GCN \mathcal{G} , initial features X^0 , task loss \mathcal{L}
1: Initialize model parameters $E^k, k \in [K], W^{K+1}$
2: **while** not converged **do**
3: Do a forward pass to compute X^k for all $k \in [K]$ as well as $\hat{\mathbf{Y}}$
4: Compute \mathbf{G} then $\frac{\partial \mathcal{L}}{\partial W^{K+1}}$ using Lemma 1 (1) and update $W^{K+1} \leftarrow W^{K+1} - \eta \cdot \frac{\partial \mathcal{L}}{\partial W^{K+1}}$
5: Compute α^K using \mathbf{G}, W^{K+1} , Lemma 1 (2)
6: **for** $k = K \dots 1$ **do**
7: Compute $\frac{\partial \mathcal{L}}{\partial E^k}$ using α^k, X^k , Lemma 1 (1)
8: Update $E^k \leftarrow E^k - \eta \cdot \frac{\partial \mathcal{L}}{\partial E^k}$
9: Update α^k using α^{k+1} using Lemma 1 (2)
10: **end for**
11: **end while**

Algorithm 2 IGLU: inverted order

Input: GCN \mathcal{G} , initial features X^0 , task loss \mathcal{L}
1: Initialize model parameters $E^k, k \in [K], W^{K+1}$
2: Do an initial forward pass to compute $X^k, k \in [K]$
3: **while** not converged **do**
4: Compute $\hat{\mathbf{Y}}, \mathbf{G}$ and α^k for all $k \in [K]$ using Lemma 1 (2)
5: **for** $k = 1 \dots K$ **do**
6: Compute $\frac{\partial \mathcal{L}}{\partial E^k}$ using α^k, X^{k-1} , Lemma 1 (1)
7: Update $E^k \leftarrow E^k - \eta \cdot \frac{\partial \mathcal{L}}{\partial E^k}$
8: Update $X^k \leftarrow f(X^{k-1}; E^k)$
9: **end for**
10: Compute $\frac{\partial \mathcal{L}}{\partial W^{K+1}}$ using Lemma 1 (1) and use it to update $W^{K+1} \leftarrow W^{K+1} - \eta \cdot \frac{\partial \mathcal{L}}{\partial W^{K+1}}$
11: **end while**

Theoretical Analysis: Note that, conditioned on the stale parameters (either α^k or X^k depending on which variant is being executed), the gradients used by IGLU to perform model updates (steps 4, 8 in Algorithm 1 and steps 7, 10 in Algorithm 2) do not exhibit any sampling bias or sampling variance. However, the staleness itself introduces bias in the training process. By controlling the step length η and the frequency with which the stale parameters are updated, this bias can be provably controlled resulting in guaranteed convergence to a first-order stationary point. Due to lack of space, we postpone the detailed statement and proof of the convergence guarantee to the appendix.

Theorem 2 (IGLU Convergence (Informal)). *Suppose the task loss function \mathcal{L} has $\mathcal{O}(1)$ -Lipschitz gradients and IGLU is executed with small enough step lengths η with model updates (steps 4, 8 in Algorithm 1 and steps 7, 10 in Algorithm 2) being carried out either in a full-batch or mini-batch SGD manner, then within T iterations, IGLU converges to a model iterate satisfying:*

1. $\|\nabla \mathcal{L}\|_2^2 \leq \mathcal{O}\left(\frac{1}{T^{\frac{2}{3}}}\right)$ if model update steps are carried out on the entire graph in a full-batch.
2. $\|\nabla \mathcal{L}\|_2^2 \leq \mathcal{O}\left(\frac{1}{\sqrt{T}}\right)$ if model update steps are carried out using mini-batch SGD.

We note that this result holds under minimal assumptions of objective smoothness and boundedness, and offers convergence rates comparable to those offered by standard mini-batch SGD. Now, typical GCN architectures use ReLU activation, which rules out smoothness assumption. But, for analysis purpose, we instead assume that the activation is a smooth function like GELU which is also shown to be similarly performant as ReLU on a variety of tasks [9].

*The backprop variant is named so since it updates model parameters in the order back-propagation would have updated them i.e. W^{K+1} followed by E^K, E^{K-1}, \dots whereas the inverted variant performs updates in the reverse order i.e. starting from E^1, E^2 all the way to W^{K+1} .

4 Empirical Evaluation

We conducted experiments on several node classification benchmarks benchmarking IGLU’s performance against key state-of-the-art (SOTA) baselines across multiple dimensions associated with GCN training such as accuracy, convergence rate and computational overheads. For IGLU, we use the inverted order of updates for our experiments and justify this choice empirically.

4.1 Datasets and Setup

Datasets: We used the following five benchmark datasets to empirically demonstrate the effectiveness of IGLU: predicting the communities to which different posts belong in Reddit [8], classifying protein functions across various biological protein-protein interaction graphs in PPI-Large, [8], categorizing types of images based on descriptions and common properties in Flickr [20], predicting paper-paper associations in OGBN-Arxiv [10] and categorizing meaningful associations between proteins in OGBN-Proteins [10]. Consistent with the original release of the datasets, we follow the same training, validation and test splits and use the same metrics originally proposed: ROC AUC for OGBN-Proteins and Micro-F1 for all the other datasets. We summarize the datasets, along with their statistics and the nature of problem considered in the appendix. The graphs we consider are varied in size (56K nodes in PPI-Large to 232K nodes in Reddit), density (average degree of 13 in OGBN-Arxiv to 597 in OGBN-Proteins) and number of edges (800K to 39 Million). They are fairly diverse in the nature of information they capture and the type of node classification tasks they solve, covering both multi-label and multi-class problems. These datasets thus enable extensive evaluation of IGLU.

Baselines: We compare IGLU with several state-of-the-art baseline algorithms, namely - GCN [13], GraphSAGE [8], VR-GCN [3], Cluster-GCN [5] and GraphSAINT [20]. In our comparisons, we use the implementation of GCN provided by GraphSAGE authors, since the full-batched version of GCN originally released by [13] runs into run time error on all the datasets. GraphSAGE and VRGCN alleviate the neighborhood explosion problem by sampling subsets of neighbors. ClusterGCN and GraphSAINT are subgraph sampling techniques, which use the sampled subgraphs for constructing convolution layers. We use the Random Walk Sampler for GraphSAINT since it is reported to have the best performance by the authors. Thus, our baselines include neighbor sampling, layer-wise sampling, subgraph sampling no-sampling methods. IGLU does not require any sampling and hence does not have additional sampling overheads. We implemented IGLU in TensorFlow, and compare with TensorFlow implementations of the baselines as released by the authors.

We note here that each of these baseline methods have a specific network architecture along with their proposed sampling strategy. We find that these architectures have additions to the standard GCN architecture [13]. This includes multiple intermediate non-linear layers, normalization layers and concatenation layers all of which can help in improving final performance and convergence. Since IGLU is architecture-agnostic, it can be readily used with any such architectures. For the experiments in this paper, we use the network architectures proposed by VR-GCN and GraphSAINT owing to their consistent performance across datasets as demonstrated in the original papers [3, 20]. We experimented with both architectures and report the results for the best performing architecture for each dataset.

Detailed Setup. We consider the inductive supervised learning setting for all the five datasets. We consider only the subgraph induced by the train nodes for training in this setting. We run experiments on PPI-Large, Reddit and Flickr datasets using 2 Layer GCNs for both IGLU and baselines and experiments on OGBN-Proteins and OGBN-Arxiv using 3 Layer GCNs for all the methods. The choice of depth of GCN’s for the OGB datasets is motivated by the depth of state-of-the art models reported in the original benchmark [10]. We implement IGLU in TensorFlow 1.15 and perform all experiments on an NVIDIA V100 GPU (32GB Memory) and Intel Xeon CPU (2.60GHz) processor.

We perform model selection for all the methods based on their performance on the validation set. We report ROC AUC score for OGBN-Proteins dataset and Micro-F1 for all the other datasets. We run each experiment five times and report the mean and standard deviation for Test Set performance in Table 1. In addition, we also compare the training times for each of these methods. Although we vary the GCN embedding dimension across the datasets, we keep them constant for a dataset across all baselines. We run all the methods on the same hardware. Additional Details regarding the implementation and baselines are mentioned in the Appendix.

Table 1: Accuracy of IGLU compared to SOTA algorithms. The metric is ROC-AUC for Proteins and Micro-F1 for the others. IGLU is the only method with accuracy within 1% of the best accuracy on each dataset. On PPI-Large, IGLU is $\sim 8\times$ faster than VR-GCN, the most accurate baseline.

Algorithm	PPI-Large	Reddit	Flickr	Proteins	Arxiv
GCN	0.614 ± 0.004	0.931 ± 0.001	0.493 ± 0.002	0.615 ± 0.004	0.657 ± 0.002
GraphSAGE	0.736 ± 0.006	0.954 ± 0.002	0.501 ± 0.013	0.759 ± 0.008	0.682 ± 0.002
VR-GCN	0.975 ± 0.007	0.964 ± 0.001	0.483 ± 0.002	0.752 ± 0.002	0.701 ± 0.006
Cluster-GCN	0.899 ± 0.004	0.962 ± 0.004	0.481 ± 0.005		0.706 ± 0.004
GraphSAINT	0.956 ± 0.003	0.966 ± 0.003	0.510 ± 0.001	0.764 ± 0.009	0.712 ± 0.006
IGLU	0.987 ± 0.004	0.963 ± 0.001	0.515 ± 0.001	0.784 ± 0.004	0.701 ± 0.002
Abs. Gain	0.012	-	0.005	0.020	-
% Speedup (1)	88.12	-	44.74	11.05	-

Hyperparameter Tuning. For IGLU, GraphSAGE and VR-GCN we perform exhaustive grid search over batch size, learning rate and dropout [15]. In addition to the standard hyperparameters: learning rate and dropout, we sweep over model specific parameters such as number of clusters for ClusterGCN and subgraph creation root and depth parameters for GraphSAINT. We also consider two different methods for normalizing the adjacency matrix. This includes the normalized laplacian matrix proposed in [13] and row normalization proposed in [21]. We report more detailed information about the hyperparameter sweeps in the Appendix.

4.2 Results

For IGLU, we empirically observe that the VR-GCN network architecture performs better for Reddit and OGBN-Arxiv datasets, while the GraphSAINT network architecture performs better for the remaining three datasets. We extensively tune all the baselines on the 5 datasets as mentioned above and are able to replicate, and in some cases, improve the reported performance numbers for the baselines. We use the higher number for comparison with IGLU. We report the test accuracy numbers in Table 1 and show the convergence plots for various methods in Figure 2. Additionally, in Table 1, we also report the absolute accuracy gain that IGLU has over the best baseline. We also quantify the % Speedup that IGLU provides as: let the highest validation score obtained by the best baseline be v_1 . Let the time taken by the corresponding baseline be t_1 . Let the time taken by IGLU to reach v_1 be t_2 . Then,

$$\% \text{ Speedup} := \frac{t_1 - t_2}{t_1} \times 100 \quad (1)$$

The wall clock training time in Figure 2 is strictly the optimization time for each method and excludes method-specific overheads such as pre-processing, sampling and sub-graph creation that other baselines incur. This is a disadvantage to IGLU since its overheads are much smaller. In the appendix we summarize the various overheads that all methods incur as well.

Performance on Test Set and Speedups Obtained: It is evident from Table 1 that IGLU significantly outperforms the baselines on 3 of the datasets, and is competitive with the baselines on the remaining two datasets. On PPI-Large, IGLU improves upon the best baseline (VRGCN) by over **1.2%** while providing speedups of upto **88%** in convergence, i.e., IGLU is about $8\times$ faster to train than VR-GCN. On OGBN-Proteins, IGLU improves upon the best baseline (GraphSAINT) by over **2.6%** while providing speedup of **11%**. On Flickr, IGLU provides upto **0.98%** improvement in performance while simultaneously offering upto **45%** speedups in convergence over the previous state-of-the-art method GraphSAINT.

The OGBN-Proteins dataset is originally benchmarked in the transductive setting, with the entire graph information made available during training. However, we consider the more challenging inductive task in our paper as described earlier, yet we outperform the best transductive baseline by over **0.7%** as reported in [10]. It is important to note that OGBN-Proteins is atypical dataset because the graph is highly dense. Because of this, baselines such as ClusterGCN and GraphSAINT that drop a lot of edges while creating subgraphs show a deterioration in performance. ClusterGCN runs into a runtime error on this dataset (denoted by || in the table), while GraphSAINT requires a very large subgraph size to achieve reasonable performance.

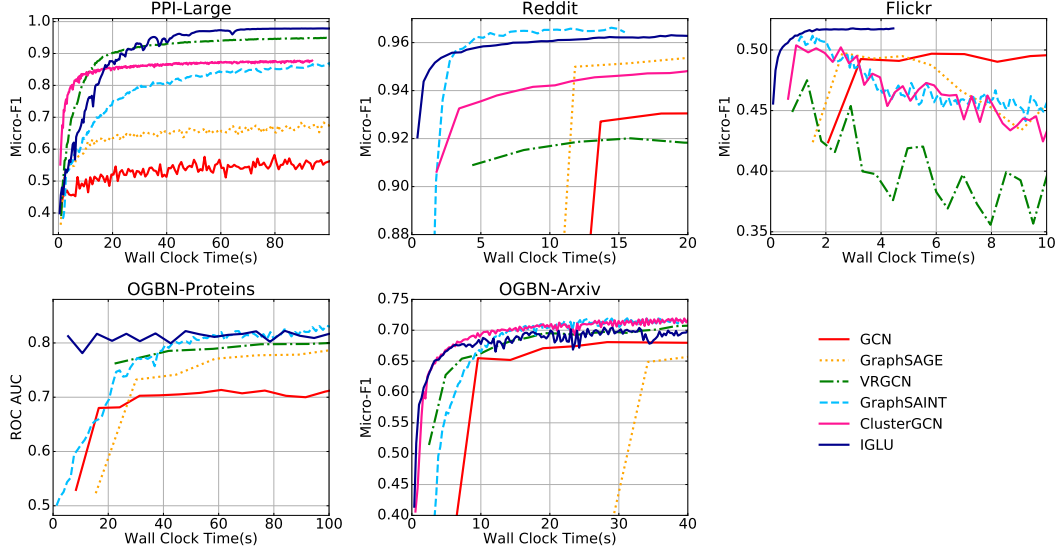


Figure 2: Wall Clock Time vs Validation Accuracy on different datasets for various methods. Clearly, IGLU offers significant improvements in convergence rate over baselines across diverse datasets.

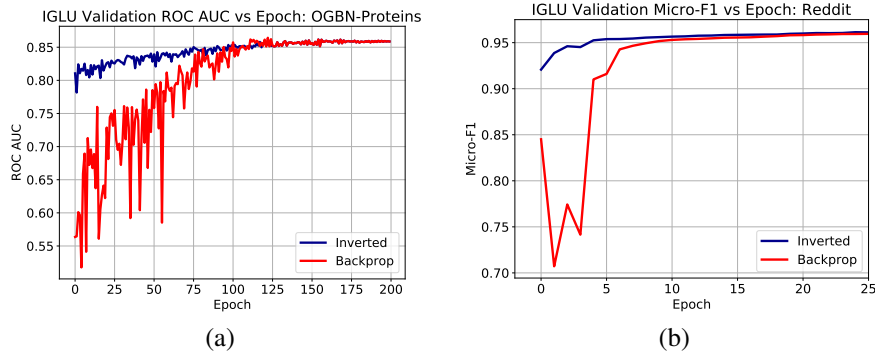


Figure 3: Effect of backpropagation and inverted order of updates in IGLU on Reddit and OGBN-Proteins datasets. Clearly, inverted order of updates offer more stability and faster convergence.

Convergence Analysis From Figure 2, we can see that IGLU converges faster to a higher validation score when compared with other baselines. In the case of PPI-Large, while Cluster-GCN and VRGCN show promising convergence in the initial stages of training, they however converge to a much lower validation score in the end, whereas IGLU is able to improve consistently and converges to a much higher validation score. In the case of Reddit, IGLU’s final validation score is only marginally lower than GraphSAINT, however, IGLU has rapid convergence in the early stages of training. For OGBN-Arxiv as well, we observe a trend very similar to Reddit, with improved convergence in the initial stages over the best baseline. For OGBN-Proteins and Flickr, IGLU demonstrates a substantial improvement in both convergence and the final performance on the test set.

4.3 Ablation studies

We provide detailed ablation studies to understand the design choices for our method while demonstrating it’s efficiency in scaling to multiple layers as compared to the other baselines.

Effect of the Order of Updates. IGLU offers the flexibility of using either the backprop order of updates or the inverted order of updates as mentioned in 3. We carefully analyse the effect of the different orders of update by performing ablations on the Reddit and OGBN-Proteins datasets. We investigate epoch-wise convergence for the same in Figure 3. It is evident that the inverted order of updates provides more stability to the algorithm and also offers improved convergence in the early stages of training. We also observe that both of the orders eventually converge to similar

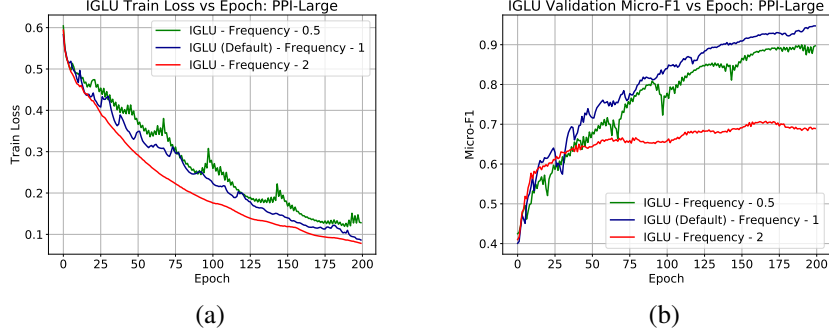


Figure 4: Update frequency vs Accuracy. Experiments conducted on PPI-Large. As expected, refreshing the α^k 's too frequently or too infrequently can affect both performance and convergence.

validation scores. Our ablations highlight the fact that the inverted order of updates accelerates the convergence and thus justifies our choice of the inverted order of updates for IGLU. In summary, we can observe that the inverted order of updates has both better convergence and consistently improving performance on the validation set. In all the ablations hereon, we will use this order of updates for our analyses.

Analysis of Degrees of Staleness. In this subsection we analyse the effect of frequency of updates to the incomplete gradients (α^k) on the performance and convergence of IGLU. We conduct our ablation by keeping all the other hyperparameters fixed. As the default setting we update all the α^k 's only once every epoch. We refer to this setting as updation with frequency 1. Apart from this scheme, we consider two different update schemes in this ablation: a) We update the α^k 's every two epochs, and b) We update the α^k 's twice within an epoch. We refer to these settings as updations with frequency 0.5 and frequency 2 respectively. To summarize, the α^k 's are the most fresh in the scheme with updation frequency 2 and they are most stale in the scheme with updation frequency 0.5. We perform this ablation study on the PPI-Large dataset. We train each variant for 200 epochs. We summarize the performance results in Table 2 by doing model selection. We plot the convergence of these variants in Figure 4. From Figure 4b, on PPI-Large dataset, we observe that IGLU with default updation frequency 1 has the best convergence on the validation set. It is followed by IGLU with updation frequency 0.5, and both these schemes significantly outperform IGLU with updation frequency 2. From Figure 4a, we observe that IGLU with updation frequency 2 has the lowest training loss, but has poor validation performance, indicating overfitting to the training dataset. We observe from this ablation that updating embeddings prematurely can cause unstable training resulting in convergence to a suboptimal solution. We observe empirically that not refreshing the α^k 's frequently enough can take the model much longer to converge to a good solution.

Table 2: Accuracy vs different update frequency on PPI-Large.

Updation Frequency	Train Micro-F1	Validation Micro-F1	Test Micro-F1
0.5	0.947	0.899	0.916
1	0.970	0.947	0.961
2	0.960	0.708	0.726

Scaling to Deeper Models. We compare the training time of IGLU with the other baselines on scaling to more convolution layers and report the detailed comparison in the Appendix.

5 Discussion and Future Work

We introduced IGLU, a new method for training general GCN type architectures. IGLU was designed based on the observation that backpropagation of gradients require *forward* pass over several nodes in the graph, which is computationally expensive. So, by a-priori storing these forward-pass embeddings, gradient descent updates could be sped up significantly, albeit by introducing bias in the updates. We argued that the bias decreases as we get closer to a stationary points, so overall convergence

is still reasonable (see Theorem 2). We validated IGLU’s performance on several datasets where it significantly outperforms SOTA methods in terms of accuracy and convergence speed. Ablation studies confirmed that IGLU is robust to its few hyperparameters to enable a near-optimal choice.

Exploring other possible variants of IGLU, in particular reducing variance due to mini-batch SGD, sampling nodes to further speed-up updates, and exploring alternate staleness schedules are interesting future directions. On a theoretical side, it would be interesting to characterize properties of datasets and loss functions that influence the effect of lazy updates on convergence. Having such a property would allow practitioners to decide whether to execute IGLU with lazier updates or else reduce the amount of staleness. Exploring application-specific uses of IGLU is also an important direction.

References

- [1] Martín Abadi, Paul Barham, Jianmin Chen, Zhifeng Chen, Andy Davis, Jeffrey Dean, Matthieu Devin, Sanjay Ghemawat, Geoffrey Irving, Michael Isard, Manjunath Kudlur, Josh Levenberg, Rajat Monga, Sherry Moore, Derek G. Murray, Benoit Steiner, Paul Tucker, Vijay Vasudevan, Pete Warden, Martin Wicke, Yuan Yu, and Xiaoqiang Zheng. Tensorflow: A system for large-scale machine learning. In *12th USENIX Symposium on Operating Systems Design and Implementation (OSDI 16)*, pages 265–283, Savannah, GA, November 2016. USENIX Association. ISBN 978-1-931971-33-1. URL <https://www.usenix.org/conference/osdi16/technical-sessions/presentation/abadi>.
- [2] Joan Bruna, Wojciech Zaremba, Arthur Szlam, and Yann LeCun. Spectral Networks and Locally Connected Networks on Graphs, 2013. arXiv:1312.6203 [cs.LG].
- [3] Jianfei Chen, Jun Zhu, and Le Song. Stochastic Training of Graph Convolutional Networks with Variance Reduction. In Jennifer Dy and Andreas Krause, editors, *Proceedings of the 35th International Conference on Machine Learning*, volume 80 of *Proceedings of Machine Learning Research*, pages 942–950. PMLR, 10–15 Jul 2018. URL <http://proceedings.mlr.press/v80/chen18p.html>.
- [4] Jie Chen, Tengfei Ma, and Cao Xiao. FastGCN: Fast Learning with Graph Convolutional Networks via Importance Sampling. In *International Conference on Learning Representations*, 2018.
- [5] Wei-Lin Chiang, Xuanqing Liu, Si Si, Yang Li, Samy Bengio, and Cho-Jui Hsieh. ClusterGCN: An Efficient Algorithm for Training Deep and Large Graph Convolutional Networks. In *Proceedings of the 25th ACM SIGKDD International Conference on Knowledge Discovery & Data Mining*, KDD ’19, page 257–266, New York, NY, USA, 2019. Association for Computing Machinery. ISBN 9781450362016. doi: 10.1145/3292500.3330925. URL <https://doi.org/10.1145/3292500.3330925>.
- [6] Cong et al. Minimal variance sampling with provable guarantees for fast training of graph neural networks. In *Proceedings of the 26th ACM SIGKDD International Conference on Knowledge Discovery & Data Mining*, KDD ’20, page 1393–1403, New York, NY, USA, 2020. Association for Computing Machinery. ISBN 9781450379984. doi: 10.1145/3394486.3403192. URL <https://doi.org/10.1145/3394486.3403192>.
- [7] Michaël Defferrard, Xavier Bresson, and Pierre Vandergheynst. Convolutional neural networks on graphs with fast localized spectral filtering. In *Proceedings of the 30th International Conference on Neural Information Processing Systems*, pages 3844–3852, 2016.
- [8] William L. Hamilton, Rex Ying, and Jure Leskovec. Inductive Representation Learning on Large Graphs, 2018.
- [9] Dan Hendrycks and Kevin Gimpel. Gaussian error linear units (gelus), 2020.
- [10] Weihua Hu, Matthias Fey, Marinka Zitnik, Yuxiao Dong, Hongyu Ren, Bowen Liu, Michele Catasta, and Jure Leskovec. Open Graph Benchmark: Datasets for Machine Learning on Graphs, 2021.
- [11] Wenbing Huang, Tong Zhang, Yu Rong, and Junzhou Huang. Adaptive Sampling Towards Fast Graph Representation Learning, 2018.
- [12] Diederik P Kingma and Jimmy Ba. Adam: A method for stochastic optimization. *arXiv preprint arXiv:1412.6980*, 2014.
- [13] Thomas N. Kipf and Max Welling. Semi-Supervised Classification with Graph Convolutional Networks, 2017.
- [14] Adam Paszke, Sam Gross, Francisco Massa, Adam Lerer, James Bradbury, Gregory Chanan, Trevor Killeen, Zeming Lin, Natalia Gimelshein, Luca Antiga, Alban Desmaison, Andreas Köpf, Edward Yang, Zach DeVito, Martin Raison, Alykhan Tejani, Sasank Chilamkurthy, Benoit Steiner, Lu Fang, Junjie Bai, and Soumith Chintala. Pytorch: An imperative style, high-performance deep learning library, 2019.

- [15] Nitish Srivastava, Geoffrey Hinton, Alex Krizhevsky, Ilya Sutskever, and Ruslan Salakhutdinov. Dropout: A simple way to prevent neural networks from overfitting. *Journal of Machine Learning Research*, 15(56):1929–1958, 2014. URL <http://jmlr.org/papers/v15/srivastava14a.html>.
- [16] Keyulu Xu, Weihua Hu, Jure Leskovec, and Stefanie Jegelka. How Powerful are Graph Neural Networks? In *International Conference on Learning Representations*, 2019.
- [17] Michihiro Yasunaga and Percy Liang. Graph-based, Self-Supervised Program Repair from Diagnostic Feedback. In *International Conference on Machine Learning (ICML)*, 2020.
- [18] Rex Ying, Ruining He, Kaifeng Chen, Pong Eksombatchai, William L. Hamilton, and Jure Leskovec. Graph convolutional neural networks for web-scale recommender systems. In *24th ACM SIGKDD International Conference on Knowledge Discovery & Data Mining (KDD)*, 2020.
- [19] Yuning You, Tianlong Chen, Zhangyang Wang, and Yang Shen. L2-GCN: Layer-Wise and Learned Efficient Training of Graph Convolutional Networks. In *Proceedings of the IEEE/CVF Conference on Computer Vision and Pattern Recognition (CVPR)*, June 2020.
- [20] Hanqing Zeng, Hongkuan Zhou, Ajitesh Srivastava, Rajgopal Kannan, and Viktor Prasanna. GraphSAINT: Graph Sampling Based Inductive Learning Method. In *International Conference on Learning Representations*, 2020. URL <https://openreview.net/forum?id=BJe8pkHFwS>.
- [21] Difan Zou, Ziniu Hu, Yewen Wang, Song Jiang, Yizhou Sun, and Quanquan Gu. Layer-Dependent Importance Sampling for Training Deep and Large Graph Convolutional Networks, 2019.

Appendix

This appendix is segmented into three key parts.

1. **Section A** discusses additional implementation details. In particular, method-specific overheads are discussed in detail and detailed hyper-parameter settings for IGLU and the main baselines reported in Table 1 are provided. A key outcome of this analysis is that IGLU has the least overheads as compared to the other methods.
2. **Section B** reports dataset statistics, provides comparisons with additional baselines (not included in the main paper due to lack of space) and provides ablation experiments on scaling to deeper models as mentioned in Section 4.3 in the main paper. The key outcome of this discussion is that IGLU scales well to, and continues to give performance boosts with, deeper models and is state-of-the-art even when compared to these additional baselines. Experimental evidence also demonstrates IGLU’s ability to better optimize learning on the train set compared to other baselines.
3. **Section C** gives detailed proofs of Lemma 1 and the convergence rates offered by IGLU. It is shown that under standard assumptions such as objective smoothness, IGLU is able to offer both the standard rate of convergence common for SGD-style algorithms, as well as a *fast* rate if full-batch GD is performed.

A Additional Implementation Details

We recall from Section 4.2 that the wall-clock time reported in Figure 2 consists of strictly the optimization time for each method and excludes method-specific overheads. This was actually a disadvantage for IGLU since its overheads are relatively mild. This section demonstrates that other baselines incur much more significant overheads whereas IGLU does not suffer from these large overheads. When included, it further improves the speedups that IGLU provides over baseline methods.

A.1 Time and Memory Overheads for Various Methods

We consider three main types of overheads that are incurred by different methods. This includes pre-processing overhead that is one-time, recurring overheads and additional memory overhead. We describe each of the overheads in the context of the respective methods below.

1. **GraphSAGE** - GraphSAGE recursively samples neighbors at each layer for every minibatch. This is done on-the-fly and contributes to a significant sampling overhead. Since this overhead is incurred for every minibatch, we categorize this under recurring overhead. We aggregate this overhead across all minibatches during training. GraphSAGE does not incur preprocessing or additional memory overheads.
2. **VRGCN** - Similar to GraphSAGE, VRGCN also recursively samples neighbors at each layer for every minibatch on-the-fly. We again aggregate this overhead across all minibatches during training. VRGCN also stores the stale/historical embeddings that are learnt for every node at every layer. This is an additional overhead of $\mathcal{O}(N K d)$, where K is the number of layers, N is the number of nodes in the graph and $d = \frac{1}{K} \sum_{k \in [K]} d_k$ is the average embedding dimensionality across layers.
3. **ClusterGCN** - ClusterGCN creates subgraphs and uses them as minibatches for training. For the creation of these subgraphs, ClusterGCN performs graph clustering using the highly optimized METIS tool[†]. This overhead is a one-time overhead since graph clustering is done before training and the same subgraphs are (re-)used during the whole training process. We categorize this under preprocessing overhead. ClusterGCN does not incur any recurring or additional memory overheads.
4. **GraphSAINT** - GraphSAINT, similar to ClusterGCN creates subgraphs to be used as minibatches for training. We categorize this minibatch creation as the preprocessing overhead for GraphSAINT. However, unlike ClusterGCN, GraphSAINT also periodically creates new

[†]<http://glaros.dtc.umn.edu/gkhome/metis/metis/download>

Table 3: **OGBN-Proteins: Overheads of different methods.** IGLU does not have any recurring overhead while VRGCN, GraphSAGE and GraphSAINT all suffer from heavy recurring overheads. ClusterGCN runs into runtime error on this dataset (**denoted by ||**). GraphSAINT incurs an overhead that is $\sim 2\times$ the overhead incurred by IGLU, while GraphSAGE and VRGCN incur upto $\sim 4.7\times$ and $\sim 7.8\times$ the overhead incurred by IGLU respectively. For the last row, I denotes initialization time, MB denotes minibatch time and T denotes total preprocessing time. Please refer to Discussion on OGBN - Proteins at Section A.1 for more details.

Method	Preprocessing (One-time)	Recurring	Additional Memory
GraphSAGE	N/A	276.8s	N/A
VRGCN	N/A	465.0s	$\mathcal{O}(NKd)$
ClusterGCN			
GraphSAINT	22.1s	101.0s	N/A
IGLU	34.0s (I) + 25.0s (MB) = 59.0s (T)	N/A	$\mathcal{O}(NKd)$

Table 4: **Reddit: Overheads of different methods.** IGLU and GraphSAINT do not have any recurring overhead for this dataset while VRGCN and GraphSAGE incur heavy recurring overheads. ClusterGCN suffers from heavy preprocessing overhead incurred due to clustering. In this case, IGLU incurs an overhead that is marginally higher ($\sim 1.4\times$) than that of GraphSAINT, while VRGCN, GraphSAGE and ClusterGCN incur as much as $\sim 2.1\times$, $\sim 4.5\times$ and $\sim 5.8\times$ the overhead incurred by IGLU respectively. For the last line, I denotes initialization time, MB denotes minibatch time and T denotes total preprocessing time. Please refer to Discussion on Reddit at Section A.1 for more details.

Method	Preprocessing (One-time)	Recurring	Additional Memory
GraphSAGE	N/A	41.7s	N/A
VRGCN	N/A	19.2s	$\mathcal{O}(NKd)$
ClusterGCN	54.0s	N/A	N/A
GraphSAINT	6.7s	N/A	N/A
IGLU	3.5s (I) + 5.7s (MB) = 9.2s (T)	N/A	$\mathcal{O}(NKd)$

subgraphs on-the-fly. We categorize this overhead incurred in creating new subgraphs as recurring overhead. GraphSAINT does not incur any additional memory overheads.

5. **IGLU** - IGLU creates mini-batches only once using subsets of nodes with their full neighborhood information which is then reused throughout the training process. In addition to this, IGLU requires initial values of both the incomplete gradients α^k and the X^k embeddings (Step 3 and first part of Step 4 in Algorithm 1 and Step 2 and Step 4 in Algorithm 2) before optimization can commence. We categorize these two overheads - mini-batch creation and initializations of α^k 's and X^k embeddings as IGLU's preprocessing overhead and note that **IGLU does not have any recurring overheads**. IGLU does incur an additional memory overhead since it needs to store the incomplete gradients α^k 's in the inverted variant and the embeddings X^k in the backprop variant. However, note that the memory occupied by X^k for a layer k is the same as that occupied by α^k for that layer (see Definition 1). Thus, for both its variants, IGLU incurs an additional memory overhead of $\mathcal{O}(NKd)$, where K is the number of layers, N is the number of nodes in the graph and $d = \frac{1}{K} \sum_{k \in [K]} d_k$ is the average embedding dimensionality across layers.

Tables 3 and 4 report the overheads incurred by different methods on the OGBN-Proteins and Reddit datasets (the largest datasets in terms of edges and nodes respectively). ClusterGCN runs into a runtime error on the Proteins dataset (**denoted by || in the table**). N/A stands for Not Applicable in the tables. In the tables, specifically for IGLU, pre-processing time is the sum of initialization time required to pre-compute α^k , X^k and mini-batch creation time. We also report the individual overhead for both initialization and mini-batch creation for IGLU. The total pre-processing time for IGLU

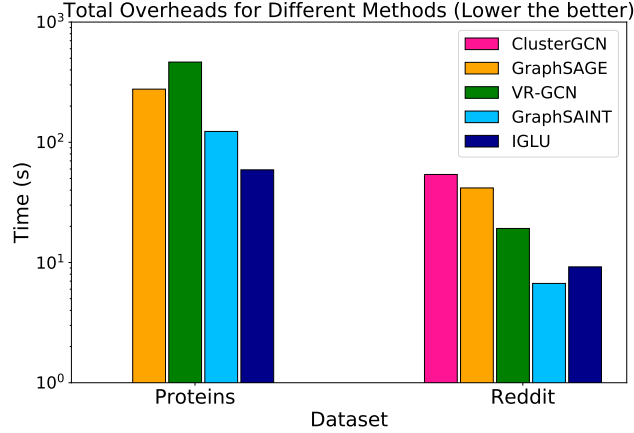


Figure 5: **Total Overheads in Wall Clock Time (Log Scale) for the different methods on OGBN-Proteins and Reddit dataset.** ClusterGCN runs into runtime error on the OGBN-Proteins dataset and hence has not been included in the plot. IGLU frequently offers least total overhead compared to the other methods and hence significantly lower overall experimentation time. Please refer to section A.1 for details.

is denoted by T , overheads incurred for initialization by I and overheads incurred for mini-batch creation by MB .

For IGLU, the minibatch creation code is currently implemented in Python, while GraphSAINT uses a highly optimized C++ implementation. Specifically for the Reddit dataset, the number of subgraphs that GraphSAINT samples initially is sufficient and it does not incur any recurring overhead. However, on Proteins, GraphSAINT samples 200 subgraphs every 18 epochs, once the initially sampled subgraphs are used, leading to a sizeable recurring overhead.

Discussion on OGBN - Proteins: Figure 5 summarizes the total overheads for all the methods. On the OGBN-Proteins dataset, IGLU incurs $\sim 2\times$ less overhead than GraphSAINT, the best baseline, while incurring as much as $\sim 7.8\times$ less overhead than VRGCN and $\sim 4.7\times$ less overhead than GraphSAGE. It is also important to note that these overheads are often quite significant as compared to the optimization time for the methods and can add to the overall experimentation time. For experiments on the OGBN-Proteins dataset, VRGCN’s total overheads equal 46.25% of its optimization time, GraphSAINT’s overheads equal 19.63% of its optimization time, GraphSAGE’s overhead equal 9.52% of its optimization time. However IGLU’s total overheads equal only **5.59%** of its optimization time which is the lowest out of all methods. Upon re-computing the speedup provided by IGLU using the formula defined in equation (1), but this time with overheads included, it was observed that IGLU offered an improved speedup of **16.88%** (the speedup was only 11.05% when considering only optimization time).

Discussion on Reddit: On the Reddit dataset, IGLU incurs upto $\sim 2.1\times$ less overhead than VRGCN and upto $\sim 4.5\times$ less overhead than GraphSAGE. However, IGLU incurs marginally higher overhead ($\sim 1.4\times$) than GraphSAINT. This can be attributed to the non-optimized minibatch creation routine currently used by IGLU compared to a highly optimized and parallelized implementation in C++ used by GraphSAINT. This is an immediate avenue for future work. Nevertheless, VRGCN’s total overhead equals 15.41% of its optimization time, GraphSAINT’s overhead equals 43.41% of its optimization time, GraphSAGE’s overhead equals 31.25% of its optimization time, ClusterGCN’s overhead equals 41.02% of its optimization time while IGLU’s overhead equals 44.09% of its optimization time. Whereas the relative overheads incurred by IGLU and GraphSAINT in comparison to optimization time may seem high for this dataset, this is because the actual optimization times for these methods are rather small, being just 15.43 and 20.86 seconds for GraphSAINT and IGLU respectively in comparison to the other methods such as VRGCN, ClusterGCN and GraphSAGE whose optimization times are 124s, 131s and 133s respectively, almost an order of magnitude larger than that of IGLU.

Table 5: URL’s and commit numbers to run baseline codes

Method	URL	Commit
GCN	github.com/williamleif/GraphSAGE	a0fdef
GraphSAGE	github.com/williamleif/GraphSAGE	a0fdef
VRGCN	github.com/thu-ml/stochastic_gcn	da7b78
ClusterGCN	github.com/google-research/google-research/tree/master/cluster_gcn	0c1bbe5
AS-GCN	github.com/huangwb/AS-GCN	5436ecd
L2-GCN	github.com/VITA-Group/L2-GCN	687fbae
MVS-GNN	github.com/CongWeilin/mvs_gcn	a29c2c5
LADIES	github.com/acbull/LADIES	c10b526

A.2 Hyperparameter Configurations for IGLU and baselines

Table 5 summarizes the source URLs and commit stamps using which baseline methods were obtained for experiments. The Adam optimizer [12] was used to train IGLU and all the baselines until convergence for each of the datasets. A grid search was performed over the other hyper-parameters for each baseline which are summarized below:

1. **GraphSAGE**: Learning Rate - {0.01, 0.001}, Batch Size - {512, 1024, 2048}, Neighborhood Sampling Size - {25, 10, 5}, Aggregator - {Mean, Concat}
2. **VRGCN** : Batch Size - {512, 1000, 2048}, Degree - {1, 5, 10}, Method - {CV, CVD}, Dropout - {0, 0.2, 0.5}
3. **ClusterGCN** : Learning Rate - {0.01, 0.001, 0.005}, Lambda - {-1, 1, 1e-4}, Number of Clusters - {5, 50, 500, 1000, 1500, 5000}, Batch Size - {1, 5, 50, 100, 500}, Dropout - {0, 0.1, 0.3, 0.5}
4. **GraphSAINT-RW** : Aggregator - {Mean, Concat}, Normalization - {Norm, Bias}, Depth - {2, 3, 4}, Root Nodes - {1250, 2000, 3000, 4500, 6000}, Dropout - {0.0, 0.2, 0.5}
5. **IGLU** : Learning Rate - {0.01, 0.001} with learning rate decay schemes, Batch Size - {512, 2048, 4096, 10000}, Dropout - {0.0, 0.2, 0.5}

B Dataset Statistics and Additional Experimental Results

B.1 Dataset Statistics

Table 6 provides details on the benchmark node classification datasets used in the experiments. The following five benchmark datasets were used to empirically demonstrate the effectiveness of IGLU: predicting the communities to which different posts belong in Reddit[‡] [8], classifying protein functions across various biological protein-protein interaction graphs in PPI-Large[§] [8], categorizing types of images based on descriptions and common properties in Flickr[¶] [20], predicting paper-paper associations in OGBN-Arxiv^{||} [10] and categorizing meaningful associations between proteins in OGBN-Proteins^{**} [10].

B.2 Comparison with additional Baselines

In addition to the baselines mentioned in Table 1, Table 7 compares IGLU to LADIES [21], L2-GCN [19], AS-GCN [11] and MVS-GNN [6] in terms of the final performance. However, a wall-clock time comparison with these methods is not provided since the author implementations of some of these methods are in PyTorch [14] which has been shown to be less efficient than Tensorflow [5, 1] for certain GCN applications. Also, the AS-GCN implementation was released by the authors for a 2 layer model only, whereas some datasets such as Proteins and Arxiv require a 3 layer model for

[‡]<http://snap.stanford.edu/graphsage/reddit.zip>

[§]<http://snap.stanford.edu/graphsage/ppi.zip>

[¶]<https://github.com/GraphSAINT/GraphSAINT> - Google Drive Link

^{||}<https://ogb.stanford.edu/docs/nodeprop/#ogbn-arxiv>

^{**}<https://ogb.stanford.edu/docs/nodeprop/#ogbn-proteins>

Table 6: **Datasets used in experiments along with their statistics.** MC refers to a multi-class problem, whereas ML refers to a multi-label problem.

Dataset	# Nodes	# Edges	Avg. Degree	# Features	# Classes	Train/Val/Test
PPI-Large	56944	818716	14	50	121 (ML)	0.79/0.11/0/10
Reddit	232965	11606919	60	602	41 (MC)	0.66/0.10/0.24
Flickr	89250	899756	10	500	7 (MC)	0.5/0.25/0.25
OGBN-Proteins	132534	39561252	597	8	112 (ML)	0.65/0.16/0.19
OGBN-Arxiv	169343	1166243	13	128	40 (MC)	0.54/0.18/0.28

Table 7: **Performance on Test Set for IGLU compared to additional algorithms.** The metric is ROC-AUC for Proteins and Micro-F1 for the others IGLU still retains the state-of-the-art results across all datasets even when compared to these new baselines. MVS-GNN ran into runtime error on the Proteins dataset (**denoted by ||**). AS-GCN ran into runtime error on datasets that require more than two layers (**denoted by ****). Please refer to section B.2 for details.

Algorithm	PPI-Large	Reddit	Flickr	Proteins	Arxiv
LADIES	0.548 ± 0.011	0.923 ± 0.008	0.488 ± 0.012	0.636 ± 0.011	0.667 ± 0.002
L2GCN	0.923 ± 0.008	0.938 ± 0.001	0.485 ± 0.001	0.531 ± 0.001	0.656 ± 0.004
ASGCN	0.687 ± 0.001	0.958 ± 0.001	0.504 ± 0.002	**	**
MVS-GNN	0.880 ± 0.001	0.950 ± 0.001	0.507 ± 0.002		0.695 ± 0.003
IGLU	0.987 ± 0.004	0.963 ± 0.001	0.515 ± 0.001	0.784 ± 0.004	0.701 ± 0.002

experimentation. Attempts to generalize the code to a 3 layer model ran into runtime errors, hence the missing results denoted by ** in Table 7. *IGLU continues to significantly outperform these additional baselines on all the datasets.*

B.3 Timing Analysis for scaling to more layers

To compare the scalability and performance of different algorithms for deeper models, models with 2, 3 and 4 layers were trained for IGLU and the baseline methods. IGLU was observed to offer a per-epoch time that scaled roughly **linearly with the number of layers** as well as offer the **highest gain in test performance as the number of layers was increased**.

B.3.1 Per Epoch Training Time

Unlike neighbor sampling methods like VRGCN and GraphSAGE, IGLU does not suffer from the neighborhood explosion problem as the number of layers increases, since IGLU updates involve only a single layer at any given time. We note that GraphSAINT and ClusterGCN also do not suffer from the neighborhood explosion problem directly since they both operate by creating GCNs on subgraphs. However, these methods may be compelled to select large subgraphs or else suffer from poor convergence. To demonstrate IGLU’s effectiveness in solving the neighborhood explosion problem, the per-epoch training times are summarized as a function of the number of layers in Table 8 on the Proteins dataset. A comparison with ClusterGCN could not be provided as since it ran into runtime errors on this dataset. In Table 8, while going from 2 to 4 layers, GraphSAINT was observed to require $\sim 1.6\times$ more time per epoch while IGLU required $\sim 2.3\times$ more time per epoch, with both methods scaling almost linearly with respect to number of layers as expected. However, GraphSAGE suffered a $\sim 62\times$ increase in time taken per epoch in this case, suffering from the neighborhood explosion problem. VRGCN ran into a run-time error for the 4 layer setting (denoted by || in Table 8). Nevertheless, even while going from 2 layers to 3 layers, VRGCN and GraphSAGE are clearly seen to suffer from the neighborhood explosion problem, resulting in an increase in training time per epoch of almost $\sim 9.4\times$ and $\sim 5.6\times$ respectively.

We note that the times for GraphSAINT in Table 8 are significantly smaller than those of IGLU even though earlier discussion reported IGLU as having the fastest convergence. However, there is no contradiction – GraphSAINT operates with very large subgraphs, with each subgraph having almost 10 % of the nodes of the entire training graph (~ 10000 nodes in a minibatch), while IGLU operates with minibatches of size 512, resulting in IGLU performing a lot more gradient updates within an epoch, as compared with GraphSAINT. Consequently, **IGLU also takes fewer epochs to converge**

Table 8: **Per epoch time (in seconds) for different methods as the number of layers increase on the OGBN-Proteins dataset.** ClusterGCN ran into a runtime error on this dataset as noted earlier. VRGCN ran into a runtime error for a 4 layer model (**denoted by II**). IGLU and GraphSAINT scale almost linearly with the number of layers. It should be noted that these times strictly include only optimization time. GraphSAINT has a much lower per-epoch time than IGLU because of the large sizes of subgraphs per batch (~ 10000 nodes), while IGLU uses minibatches of size of 512. This results in far less gradient updates within an epoch for GraphSAINT when compared with IGLU, resulting in a much smaller per-epoch time but requiring more epochs overall. Please refer to section B.3.1 for details.

Method	Number of Layers		
	2	3	4
GraphSAGE	2.6	14.5	163.1
VR-GCN	2.3	21.5	II
GraphSAINT	0.45	0.61	0.76
IGLU	2.97	5.27	6.99

Table 9: **Test Performance (ROC-AUC) at Best Validation for different methods as the number of layers increase on the OGBN-Proteins Dataset.** Results are reported for a single run but trends were observed to remain consistent across repeated runs. VRGCN ran into runtime error for 4 layers (**denoted by II**). IGLU offers steady increase in performance as the number of layers increase, as well as state-of-the-art performance throughout. GraphSAGE shows a decrease in performance on moving from 3 to 4 layers while GraphSAINT shows only a marginal increase in performance. Please refer to section B.3.2 for details.

Method	Number of Layers		
	2	3	4
GraphSAGE	0.755	0.759	0.742
VR-GCN	0.732	0.749	II
GraphSAINT	0.752	0.764	0.767
IGLU	0.768	0.783	0.794

to a better solution than GraphSAINT, thus compensating for the differences in time taken per epoch.

B.3.2 Test Convergence AUC

This section explores the effect of increasing the number of layers on convergence rate, optimization time, and final accuracy, when scaling to larger number of layers. To jointly estimate the efficiency of a method in terms of wall clock time and test performance achieved, the area under the test convergence plots (AUTC) for various methods was computed. A method that converged rapidly and that too to better performance levels would have a higher AUTC than a method that converges to suboptimal values or else converges very slowly. To fairly time all methods, each method was offered time that was triple of the time it took the best method to reach its highest validation score. Defining the cut-off time this way ensures that methods that may not have rapid early convergence still get a fair chance to improve by having better final performance, while also simultaneously penalizing methods that may have rapid early convergence but poor final performance. We rescale the wall clock time to be between 0 and 1, where 0 refers to the start of training while 1 refers to the cut-off time.

Results: Figure 6 summarizes the AUTC values. IGLU consistently obtains higher AUC values than all methods for all number of layers demonstrating its stability, rapid convergence during early phases of training and ability to generalize better as compared to other baselines. GraphSAGE suffered from neighborhood explosion leading to increased training times and hence decreased AUC values as the

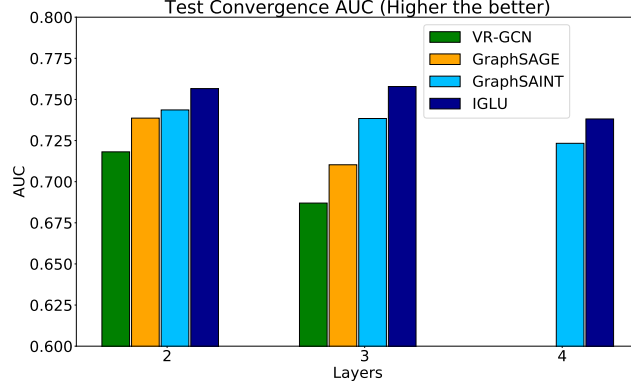


Figure 6: **Test Convergence AUC plots across different number of layers on the OGBN-Proteins dataset.** IGLU has consistently higher AUC values compared to the other baselines, demonstrating increased stability, faster convergence and better generalization. GraphSAGE suffers from neighborhood explosion problem and the training became very slow as noted earlier. This results in a decrease in the AUC while going from 3 to 4 layers. GraphSAGE’s AUC for 4 layers is only 0.313, and is thus not visible in the plot. VRGCN also suffers from the neighborhood explosion problem and runs into runtime errors for a 4 layer model. ClusterGCN runs into runtime error for the OGBN-Proteins for all of 2, 3 and 4 layers and is therefore not present in this analysis. Please refer to Section B.3.2 for details.

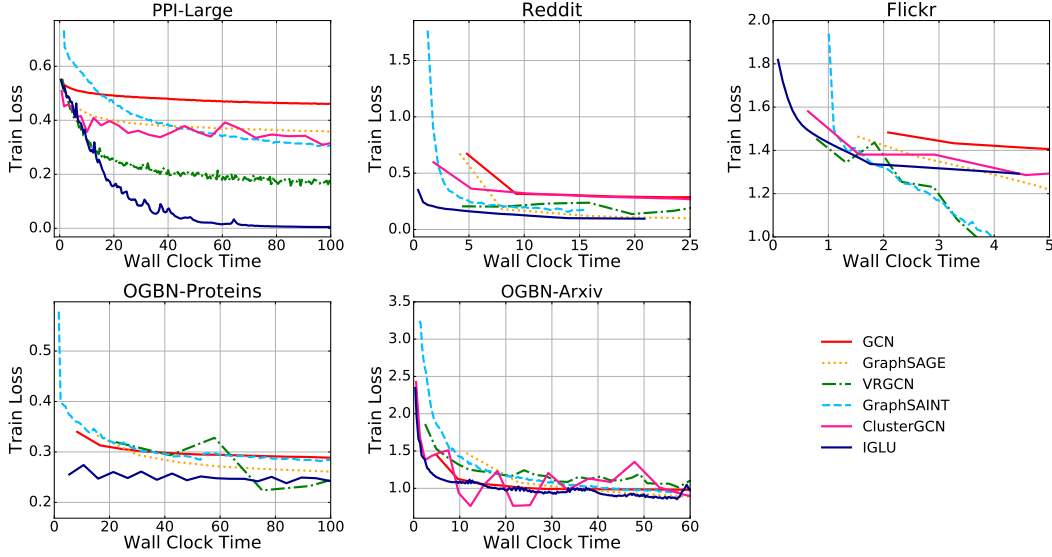


Figure 7: **Training Loss curves of different methods on the benchmark datasets against Epochs.** IGLU is able to optimize the learning on the train set better than all the other baselines across diverse datasets.

number of layers increase. VR-GCN also suffered from the same issue, and additionally ran into a run-time error for 4 layer models.

Test Performance with Increasing Layers: Table 9 summarizes the final test performances for different methods, across different number of layers. The performance for some methods is inconsistent as the depth increases whereas *IGLU* consistently outperforms all the baselines in this case as well with gains in performance as we increase the number of layers hence making it an attractive technique to train deeper GCN models.

B.4 Convergence - Train Loss vs Wall Clock Time

Figure 7 provides train loss curves for all datasets and methods in Table 1. IGLU is able to optimize train set loss significantly better than all the other baselines on multiple diverse datasets.

C Theoretical Proofs

In this section we provide a formal restatement of Theorem 2 as well as its proof. We also provide the proof of Lemma 1 below.

C.1 Proof for Lemma 1

Proof of Lemma 1 We consider the two parts of Lemma 1 separately and consider two cases while proving each part. For each part, Case 1 pertains to the final layer and Case 2 considers intermediate layers. Below we discuss why the use of α is correct.

Clarification about some Notation in the statements of Definition 1 and Lemma 1: The notation $\left. \frac{\partial(G \odot \hat{Y})}{\partial X_{jp}^k} \right|_G$ is meant to denote the partial derivative w.r.t X_{jp}^k but while keeping G fixed i.e. treated as a constant or being “conditioned upon” (indeed both G and \hat{Y} depend on X_{jp}^k but the definition keeps G fixed while taking derivatives). Similarly, in Lemma 1 part 1, α^k is fixed (treated as a constant) in the derivative in the definition of $\partial \mathcal{L} / \partial E^k$ and in part 2, α^{k+1} is fixed (treated as a constant) in the derivative in the definition of α^k .

Recalling some Notation for sake of completeness: We recall that x_i^k is the k -th layer embedding of node i . y_i is the C -dimensional ground-truth label vector for node i and \hat{y}_i is the C -dimensional predicted score vector for node i . K is total number of layers in the GCN. \mathcal{L}_i denotes the loss on the i -th node and \mathcal{L} denotes the total loss summed over all nodes. d_k is the embedding dimensionality after the k -th layer.

Appropriateness of the definition of α : Lets take a toy chain rule application to illustrate the point: if $x = f(y)$ and $y = g(z)$, chain rule tells us that $\frac{\partial x}{\partial z} = \frac{\partial x}{\partial y} \frac{\partial y}{\partial z} = g \cdot \frac{\partial y}{\partial z}$ if we use the shorthand $g := \frac{\partial x}{\partial y}$. Another way of writing this is $\left. \frac{\partial x}{\partial z} = \frac{\partial(g \cdot y)}{\partial z} \right|_g$ which treats g as a constant while taking derivatives as per our notational convention. Derivatives of the form $\frac{\partial g}{\partial z}$ do not participate in the calculation of $\frac{\partial x}{\partial z}$ even though g may very well depend on z . An identical discussion applies to the definition of α^k as well. We notice that the definition of α^k emerges naturally when attempting to analyze $\frac{\partial \mathcal{L}}{\partial E^k}$ in our proof of Lemma 1.1 (case 2) below. In the proof, we will see that we get

$$\frac{\partial \mathcal{L}}{\partial E^k} = \sum_{i=1}^N \sum_{c \in [C]} g_{ic} \cdot \sum_{j=1}^N \sum_{p=1}^{d_k} \frac{\partial \hat{y}_{ic}}{\partial X_{jp}^k} \frac{\partial X_{jp}^k}{\partial E^k} = \sum_{j=1}^N \sum_{p=1}^{d_k} \left(\sum_{i=1}^N \sum_{c \in [C]} g_{ic} \cdot \frac{\partial \hat{y}_{ic}}{\partial X_{jp}^k} \right) \frac{\partial X_{jp}^k}{\partial E^k},$$

where the term within the round braces is nothing but α_{jp}^k . We see that this makes it natural to condition on g_{ic} and treat it as a constant while taking derivatives and justifies why the definition of α^k is correct. Moreover, the proofs below show that the chosen definitions do give us the correct loss derivatives, as well as they allow us to obtain a nice recursive definition of α^k in terms of α^{k+1} .

Proof of Lemma 1.1 We analyze two cases

Case 1 ($k = K$ i.e. final layer): Recall that the predictions for node i are obtained as $\hat{y}_i = (W^{K+1})^\top x_i^K$. Thus we have

$$\frac{\partial \mathcal{L}}{\partial W^{K+1}} = \sum_{i=1}^N \sum_{c \in [C]} \frac{\partial \mathcal{L}_i}{\partial \hat{y}_{ic}} \frac{\partial \hat{y}_{ic}}{\partial W^{K+1}}.$$

Now, $\frac{\partial \mathcal{L}_i}{\partial \hat{y}_{ic}} = g_{ic}$ by definition. If we let w_c^{K+1} denote the c -th column of the $d_k \times C$ matrix W^{K+1} , then it is clear that \hat{y}_{ic} depends only on w_c^{K+1} and x_i^K . Thus, we have

$$\frac{\partial \hat{y}_{ic}}{\partial W^{K+1}} = \frac{\partial \hat{y}_{ic}}{\partial w_c^{K+1}} \cdot e_c^\top = (x_i^K)^\top e_c^\top,$$

where e_c is the c -th canonical vector in C -dimensions with 1 at the c -th coordinate and 0 everywhere else. This gives us

$$\frac{\partial \mathcal{L}}{\partial W^{K+1}} = \sum_{i=1}^N (x_i^K)^\top \sum_{c \in [C]} g_{ic} \cdot e_c^\top = (X^K)^\top G$$

Case 2 ($k < K$ i.e. intermediate layers): We recall that X^k stacks all k -th layer embeddings as an $N \times d_k$ matrix and $X^k = f(X^{k-1}; E^k)$ where E^k denotes the parameters (weights, offsets, scales) of the k -th layer. Thus we have

$$\frac{\partial \mathcal{L}}{\partial E^K} = \sum_{i=1}^N \sum_{c \in [C]} \frac{\partial \mathcal{L}}{\partial \hat{y}_{ic}} \frac{\partial \hat{y}_{ic}}{\partial E^K}.$$

As before, $\frac{\partial \mathcal{L}}{\partial \hat{y}_{ic}} = g_{ic}$ by definition and we have

$$\frac{\partial \hat{y}_{ic}}{\partial E^K} = \sum_{j=1}^N \sum_{p=1}^{d_k} \frac{\partial \hat{y}_{ic}}{\partial X_{jp}^k} \frac{\partial X_{jp}^k}{\partial E^K}$$

This gives us

$$\frac{\partial \mathcal{L}}{\partial E^K} = \sum_{i=1}^N \sum_{c \in [C]} g_{ic} \cdot \sum_{j=1}^N \sum_{p=1}^{d_k} \frac{\partial \hat{y}_{ic}}{\partial X_{jp}^k} \frac{\partial X_{jp}^k}{\partial E^K} = \sum_{j=1}^N \sum_{p=1}^{d_k} \alpha_{jp}^k \cdot \frac{\partial X_{jp}^k}{\partial E^K} = \left. \frac{\partial (\alpha^k \odot X^k)}{\partial E^k} \right|_{\alpha^k},$$

where we used the definition of α_{jp}^k in the second step and used a “conditional” notation to get the third step. We reiterate that $\left. \frac{\partial (\alpha^k \odot X^k)}{\partial E^k} \right|_{\alpha^k}$ implies that α^k is fixed (treated as a constant) while taking the derivative. This “conditioning” is critical since α^k also depends on E^k . This concludes the proof.

Proof of Lemma 1.2: We consider two cases yet again and use Definition 1 that tells us that

$$\alpha_{jp}^k = \sum_{i \in \mathcal{V}} \sum_{c \in [C]} g_{ic} \cdot \frac{\partial \hat{y}_{ic}}{\partial X_{jp}^k} = \sum_{i=1}^N \sum_{c \in [C]} g_{ic} \cdot \frac{\partial \hat{y}_{ic}}{\partial X_{jp}^k}$$

Case 1 ($k = K$): Since $\hat{y}_i = (W^{K+1})^\top x_i^K$, we know that \hat{y}_{ic} depends only on x_i^K and w_c^{K+1} where as before, w_c^{K+1} is the c -th column of the matrix W^{K+1} . This gives us $\frac{\partial \hat{y}_{ic}}{\partial X_{jp}^K} = 0$ if $i \neq j$ and $\frac{\partial \hat{y}_{ic}}{\partial X_{jp}^K} = w_{pc}^K$ if $i = j$ where w_{pc}^K is the (p, c) -th entry of the matrix W^{K+1} (or in other words, the p -th coordinate of the vector w_c^{K+1}). This tells us that

$$\alpha_{jp}^K = \sum_{i=1}^N \sum_{c \in [C]} g_{ic} \cdot \frac{\partial \hat{y}_{ic}}{\partial X_{jp}^K} = \sum_{c \in [C]} g_{jc} \cdot w_{pc}^K,$$

which gives us $\alpha^K = G(W^{K+1})^\top$.

Case 2 ($k < K$): By Definition 1 we have

$$\alpha_{jp}^k = \sum_{i=1}^N \sum_{c \in [C]} g_{ic} \cdot \frac{\partial \hat{y}_{ic}}{\partial X_{jp}^k} = \sum_{i=1}^N \sum_{c \in [C]} g_{ic} \cdot \sum_{l=1}^N \sum_{q=1}^{d_{k+1}} \frac{\partial \hat{y}_{ic}}{\partial X_{lq}^{k+1}} \frac{\partial X_{lq}^{k+1}}{\partial X_{jp}^k}$$

Rearranging the terms gives us

$$\alpha_{jp}^k = \sum_{l=1}^N \sum_{q=1}^{d_{k+1}} \left(\sum_{i=1}^N \sum_{c \in [C]} g_{ic} \cdot \frac{\partial \hat{y}_{ic}}{\partial X_{lq}^{k+1}} \right) \cdot \frac{\partial X_{lq}^{k+1}}{\partial X_{jp}^k} = \sum_{l=1}^N \sum_{q=1}^{d_{k+1}} \alpha_{lq}^{k+1} \cdot \frac{\partial X_{lq}^{k+1}}{\partial X_{jp}^k},$$

where we simply used Definition 1 in the second step. However, the resulting term is simply $\left. \frac{\partial (\alpha^{k+1} \odot X^{k+1})}{\partial X_{jp}^k} \right|_{\alpha^{k+1}}$ which conditions on, or treats as a constant, the term α^{k+1} according to our notational convention. This finishes the proof of part 2.

C.2 Statement of Convergence Guarantee

The rate for full-batch updates, as derived below, is $\mathcal{O}\left(\frac{1}{T^{\frac{2}{3}}}\right)$. This *fast* rate offered by full-batch updates is asymptotically superior to the $\mathcal{O}\left(\frac{1}{\sqrt{T}}\right)$ rate offered by mini-batch SGD updates. This is due to the additional variance due to mini-batch construction that mini-batch SGD variants have to incur.

Theorem 3 (IGLU Convergence (Final)). *Suppose the task loss function \mathcal{L} has H -smooth and an architecture that offers bounded gradients and Lipschitz gradients as quantified below, then if IGLU in its inverted variant (Algorithm 2) is executed with step length η and a staleness count of τ updates per layer as in steps 7, 10 in Algorithm 2, then within T iterations, we must have*

1. $\|\nabla \mathcal{L}\|_2^2 \leq \mathcal{O}\left(1/T^{\frac{2}{3}}\right)$ if model update steps are carried out on the entire graph in a full-batch with step length $\eta = \mathcal{O}\left(1/T^{\frac{1}{3}}\right)$ and $\tau = \mathcal{O}(1)$.
2. $\|\nabla \mathcal{L}\|_2^2 \leq \mathcal{O}\left(1/\sqrt{T}\right)$ if model update steps are carried out using mini-batch SGD with step length $\eta = \mathcal{O}\left(1/\sqrt{T}\right)$ and $\tau = \mathcal{O}\left(T^{\frac{1}{4}}\right)$.

Our overall proof strategy is the following

1. **Step 1:** Analyze how lazy updates in IGLU affect model gradients
2. **Step 2:** Bound the bias in model gradients in terms of staleness due to the lazy updates
3. **Step 3:** Using various properties such as smoothness and boundedness of gradients, obtain an upper bound for the bias in the gradients in terms of number of iterations since last update
4. **Step 4:** Using the above to establish the convergence guarantees

We will show the results for the variant of IGLU that uses the *inverted* order of updates as given in Algorithm 2. A similar proof technique will also work for the variant that uses the *backprop* order of updates. Also, to avoid clutter, we will from hereon assume that a normalized total loss function is used for training i.e. $\mathcal{L} = \frac{1}{N} \sum_{i \in \mathcal{V}} \ell_i$ where $N = |\mathcal{V}|$ is the number of nodes in the training graph.

C.3 Step 1: Partial Staleness and its Effect on Model Gradients

A peculiarity of the inverted order of updates is that the embeddings $X^k, k \in [K]$ are never stale in this variant. To see this, we use a simple inductive argument. The base case is X^0 that is never stale since it is never updated. For the inductive case, notice how, the moment any parameter E^k is updated in step 7 of Algorithm 2 (whether by mini-batch SGD or by full-batch GD), immediately thereafter in step 8 of the algorithm, X^k is updated using the current value of X^{k-1} and E^k . Since by induction X^{k-1} never has a stale value, this shows that X^k is never stale either, completing the inductive argument.

This has an interesting consequence. Notice that by Lemma 1, we have $\frac{\partial \mathcal{L}}{\partial E^k} = \frac{1}{N} \frac{\partial(\alpha^k \odot X^k)}{\partial E^k} \Big|_{\alpha^k}$ (notice the additional $1/N$ term since we are using a normalized total loss function now). However, as $\frac{\partial(\alpha^k \odot X^k)}{\partial E^k} \Big|_{\alpha^k}$ is completely defined given E^k, α^k and X^{k-1} and by the above argument, X^{k-1} never has a stale value. This shows that the only source of staleness in $\frac{\partial \mathcal{L}}{\partial E^k}$ is the staleness in values of the incomplete task gradient α^k . Similarly, it is easy to see that the only source of staleness in $\frac{\partial \mathcal{L}}{\partial W^{K+1}} = (X^K)^\top \mathbf{G}$ is the staleness in \mathbf{G} .

The above argument is easily mirrored for the backprop order of updates where an inductive argument similar to the one used to argue above that X^k values are never stale in the inverted update variant, would show that the incomplete task gradient α^k values are never stale in the backprop variant and the only source of staleness in $\frac{\partial \mathcal{L}}{\partial E^k}$ would then be the staleness in the X^k values.

C.4 Relating the Bias in Model Gradients to Staleness

The above argument allows us to bound the bias in model gradients as a result of lazy updates. To avoid clutter, we will present the arguments with respect to the E^k parameter. Similar arguments would hold for the W^{K+1} parameter as well. Let $\tilde{\alpha}^k, \alpha^k$ denote the stale and current values of the incomplete task gradient relevant to E^k . Let $\frac{\partial \tilde{\mathcal{L}}}{\partial E^k} = \frac{\partial(\tilde{\alpha}^k \odot X^k)}{\partial E^k} \Big|_{\tilde{\alpha}^k}$ be the stale gradients used by IGLU in its inverted variant to update E^k and similarly let $\frac{\partial \mathcal{L}}{\partial E^k} = \frac{\partial(\alpha^k \odot X^k)}{\partial E^k} \Big|_{\alpha^k}$ be the true gradient that could have been used had there been no staleness.

We will abuse notation and let the vectorized forms of these incomplete task gradients be denoted by the same symbols i.e. we stretch the matrix $\alpha^k \in \mathbb{R}^{N \times d_k}$ into a long vector denoted also by $\alpha^k \in \mathbb{R}^{N \cdot d_k}$. Let $\dim(E^k)$ denote the number of dimensions in the model parameter E^k (recall that E^k can be a stand-in for weight matrices, layer norm parameters etc used in layer k of the GCN). Similarly, we let $Z_{jp}^k \in \mathbb{R}^{\dim(E^k)}, j \in [N], p \in [d_k]$ denote the vectorized form of the gradient $\frac{\partial X_{ip}^k}{\partial E^k}$ and let $Z^k \in \mathbb{R}^{N \cdot d_k \times \dim(E^k)}$ denote the matrix with all these vectors Z_{jp}^k stacked up.

As per the above notation, it is easy to see that the vectorized form of the model gradient is given by

$$\frac{\partial \mathcal{L}}{\partial E^k} = \frac{(Z^k)^\top \alpha^k}{N} \in \mathbb{R}^{\dim(E^k)}$$

Yet again, notice the $1/N$ term since we are using a normalized total loss function. This also tells us that

$$\left\| \frac{\partial \tilde{\mathcal{L}}}{\partial E^k} - \frac{\partial \mathcal{L}}{\partial E^k} \right\|_2 = \frac{\sqrt{(\tilde{\alpha}^k - \alpha^k)^\top (Z^k (Z^k)^\top) (\tilde{\alpha}^k - \alpha^k)}}{N} \leq \frac{\|\tilde{\alpha}^k - \alpha^k\|_2 \cdot \sigma_{\max}(Z^k)}{N},$$

where $\sigma_{\max}(Z^k)$ is the largest singular value of the matrix Z^k .

C.5 Step 3: Smoothness and Bounded Gradients to Bound Gradient Bias

The above discussion shows how to bound the bias in gradients in terms of staleness in the incomplete task gradients. However, to utilize this relation, we assume that the loss function \mathcal{L} is H -smooth which is a standard assumption in literature. We will also assume that the network offers bounded gradients.

Specifically, for all values of model parameters $E^k, k \in [K], W^{K+1}$ we have $\left\| \frac{\partial X_{ip}^k}{\partial E^k} \right\|_2, \left\| \frac{\partial \mathcal{L}}{\partial E^k} \right\|_2 \leq B$. Assuming bounded gradients is also standard in literature. However, whereas works such as [3] assume bounds on the sup-norm i.e. $\|\cdot\|_\infty$ of the gradients, our proofs only require an L_2 norm bound.

We note that the H -smoothness of the task loss automatically grants us Lipschitz gradients. Thus, if the model parameters $\tilde{E}^k, k \in [K], \tilde{W}^{K+1}$ undergo gradient updates to their new values $E^k, k \in [K], W^{K+1}$ and the amount of *travel* is bounded by $r > 0$ i.e. $\|\tilde{E}^k - E^k\|_2 \leq r$ and so on, then we have $\|\tilde{\alpha}^k - \alpha^k\|_2 \leq I \cdot r$ where $\tilde{\alpha}^k, \alpha^k$ are the incomplete task gradients corresponding to respectively old and new model parameter values and I depends on various quantities such as H and the number of layers in the network.

The above tells us that in Algorithm 2, suppose the parameter update steps i.e. step 7 and step 10 are executed by effecting τ mini-batch SGD steps or else τ full-batch GD steps each time, with step length η , then the amount of travel in any model parameter is bounded above by $\tau\eta B$ i.e. $\|\tilde{E}^k - E^k\|_2 \leq \tau\eta B$ and so on. Now, incomplete task gradients α^k are updated only after model parameters for all layers have been updated once and the algorithm loops back to step 6. Thus, Lipschitzness of the gradients tells us that the staleness in the incomplete task gradients, for any $k \in [K]$, is upper bounded by

$$\|\tilde{\alpha}^k - \alpha^k\|_2 \leq \tau\eta \cdot IB$$

Now, since $\left\| \frac{\partial X_{ip}^k}{\partial E^k} \right\|_2 \leq B$ we have $\sigma_{\max}(Z^k) \leq N \cdot d_k B$. This gives us

$$\left\| \frac{\partial \widetilde{\mathcal{L}}}{\partial E^k} - \frac{\partial \mathcal{L}}{\partial E^k} \right\|_2 \leq \tau \eta \cdot IB^2 d_k$$

Taking in contributions of gradients of all layers and the final classifier layer gives us the bias in the total gradient using triangle inequality as

$$\left\| \widetilde{\nabla \mathcal{L}} - \nabla \mathcal{L} \right\|_2 \leq \sum_{k \in [K]} \left\| \frac{\partial \widetilde{\mathcal{L}}}{\partial E^k} - \frac{\partial \mathcal{L}}{\partial E^k} \right\|_2 + \left\| \frac{\partial \widetilde{\mathcal{L}}}{\partial W^{K+1}} - \frac{\partial \mathcal{L}}{\partial W^{K+1}} \right\|_2 \leq \tau \eta \cdot IB^2 d_{\max}(K+1),$$

where $d_{\max} = \max_{k \in K} d_k$ is the maximum embedding dimensionality of any layer.

C.6 Step 4 (i): Convergence Guarantee (mini-batch SGD)

Let us analyze convergence in the case when updates are made using mini-batch SGD in steps 7, 10 of Algorithm 2. The discussion above establishes an upper bound on the *absolute* bias in the gradients. However, our proofs later require a *relative* bound which we tackle now. Let us decide to set the step length to $\eta = \frac{1}{C\sqrt{T}}$ for some constant $C > 0$ that will be decided later and also set some value $\phi < 1$. Then two cases arise

1. **Case 1:** The relative gradient bias is too large i.e. $\tau \eta \cdot IB^2 d_{\max}(K+1) > \phi \cdot \|\nabla \mathcal{L}\|_2$. In this case we are actually done since we get

$$\|\nabla \mathcal{L}\|_2 \leq \frac{\tau \cdot IB^2 d_{\max}(K+1)}{\phi \cdot C\sqrt{T}},$$

i.e. we are already at an approximate first-order stationary point.

2. **Case 2:** The relative gradient bias is small i.e. $\tau \eta \cdot IB^2 d_{\max}(K+1) \leq \phi \cdot \|\nabla \mathcal{L}\|_2$. In this case we satisfy the relative bias bound required by Lemma 4 (part 2) with $\delta = \phi$.

This shows that either Case 1 happens in which case we are done or else Case 2 keeps applying which means that Lemma 4 (part 2) keeps getting its prerequisites satisfied. If Case 1 does not happen for T steps, then Lemma 4 (part 2) assures us that we will arrive at a point where

$$\mathbb{E} \left[\|\nabla \mathcal{L}\|_2^2 \right] \leq \frac{2C(\mathcal{L}^0 - \mathcal{L}^*) + H\sigma^2/C}{(1 - \phi)\sqrt{T}}$$

where $\mathcal{L}^0, \mathcal{L}^*$ are respectively the initial and optimal values of the loss function which we recall is H -smooth and σ^2 is the variance due to mini-batch creation and we set $\eta = \frac{1}{C\sqrt{T}}$. Setting

$C = \sqrt{\frac{H\sigma^2}{2(\mathcal{L}^0 - \mathcal{L}^*)}}$ tells us that within T steps, either we will achieve

$$\|\nabla \mathcal{L}\|_2^2 \leq \frac{2\tau^2 \cdot I^2 B^4 d_{\max}^2 (K+1)^2 (\mathcal{L}^0 - \mathcal{L}^*)}{\phi^2 H \sigma^2 T},$$

or else we will achieve

$$\mathbb{E} \left[\|\nabla \mathcal{L}\|_2^2 \right] \leq \frac{2\sigma \sqrt{2(\mathcal{L}^0 - \mathcal{L}^*)} H}{(1 - \phi)\sqrt{T}}$$

Setting $\tau = T^{\frac{1}{4}} \cdot \left(\frac{\sqrt{\sigma^3 H \sqrt{H}}}{(\mathcal{L}^0 - \mathcal{L}^*)^{\frac{1}{4}} IB^2 d_{\max}(K+1)} \right)$ balances the two quantities in terms of their dependence on T upto dependence on absolute constants such as ϕ . Note that as expected, as the quantities I, B, d_{\max}, K increase, the above limit on τ goes down i.e. we are able to perform fewer and fewer updates to the model parameters before a refresh is required. This concludes the proof of Theorem 3 for the second case.

C.7 Step 4 (ii): Convergence Guarantee (full-batch GD)

In this case we similarly have either the relative gradient bias to be too large in which case we get

$$\|\nabla \mathcal{L}\|_2 \leq \frac{\tau\eta \cdot IB^2 d_{\max}(K+1)}{\phi},$$

or else we satisfy the relative bias bound required by Lemma 4 (part 1) with $\delta = \phi$. This shows that either Case 1 happens in which case we are done or else Case 2 keeps applying which means that Lemma 4 (part 1) keeps getting its prerequisites satisfied. If Case 1 does not happen for T steps, then Lemma 4 (part 1) assures us that we will arrive at a point where

$$\|\nabla \mathcal{L}\|_2^2 \leq \frac{2(\mathcal{L}^0 - \mathcal{L}^*)}{\eta(1-\phi)T}$$

In this case, for a given value of τ , setting $\eta = \left(\frac{2(\mathcal{L}^0 - \mathcal{L}^*)}{(1-\phi)\tau^2 I^2 B^4 d_{\max}^2 (K+1)^2 T} \right)^{\frac{1}{3}}$ gives us that within T iterations, we must achieve

$$\|\nabla \mathcal{L}\|_2^2 \leq \left(\frac{2\tau(\mathcal{L}^0 - \mathcal{L}^*)IB^2 d_{\max}(K+1)}{(1-\phi)} \right)^{\frac{2}{3}} \cdot \frac{1}{T^{\frac{2}{3}}}$$

In this case, it is prudent to set $\tau = \mathcal{O}(1)$ so as to not deteriorate the convergence rate. This concludes the proof of Theorem 3 for the first case.

C.8 Generic Convergence Guarantee

Lemma 4 (First-order Stationarity with a Smooth Objective). *Let $f : \Theta \rightarrow \mathbb{R}$ be a H -smooth objective over model parameters $\theta \in \Theta$ that is being optimized using a gradient oracle and the following update for step length η :*

$$\theta^{t+1} = \theta^t - \eta \cdot \mathbf{g}^t$$

Let θ^ be an optimal point i.e. $\theta^* \in \arg \min_{\theta \in \Theta} f(\theta)$. Then, the following results hold depending on the nature of the gradient oracle:*

1. *If a non-stochastic gradient oracle with bounded bias is used i.e. for some $\delta \in (0, 1)$, for all t , we have $\mathbf{g}^t = \nabla f(\theta^t) + \Delta^t$ where $\|\Delta^t\|_2 \leq \delta \cdot \|\nabla f(\theta^t)\|_2$ and if the step length satisfies $\eta \leq \frac{(1-\delta)}{2H(1+\delta^2)}$, then for any $T > 0$, for some $t \leq T$ we must have*

$$\|\nabla f(\theta^t)\|_2^2 \leq \frac{2(f(\theta^0) - f(\theta^*))}{\eta(1-\delta)T}$$

2. *If a stochastic gradient oracle is used with bounded bias i.e. for some $\delta \in (0, 1)$, for all t , we have $\mathbb{E}[\mathbf{g}^t | \theta^t] = \nabla f(\theta^t) + \Delta^t$ where $\|\Delta^t\|_2 \leq \delta \cdot \|\nabla f(\theta^t)\|_2$, as well as bounded variance i.e. for all t , we have $\mathbb{E}[\|\mathbf{g}^t - \nabla f(\theta^t) - \Delta^t\|_2^2 | \theta^t] \leq \sigma^2$ and if the step length satisfies $\eta \leq \frac{(1-\delta)}{2H(1+\delta^2)}$, as well as $\eta = \frac{1}{C\sqrt{T}}$ for some $C > 0$, then for any $T > \frac{4H^2(1+\delta^2)^2}{C^2(1-\delta)^2}$, for some $t \leq T$ we must have*

$$\mathbb{E}[\|\nabla f(\theta^t)\|_2^2] \leq \frac{2C(f(\theta^0) - f(\theta^*)) + H\sigma^2/C}{(1-\delta)\sqrt{T}}$$

Proof (of Lemma 4). To prove the first part, we notice that smoothness of the objective gives us

$$f(\theta^{t+1}) \leq f(\theta^t) + \langle \nabla f(\theta^t), \theta^{t+1} - \theta^t \rangle + \frac{H}{2} \|\theta^{t+1} - \theta^t\|_2^2$$

Since we used the update $\theta^{t+1} = \theta^t - \eta \cdot \mathbf{g}^t$ and we have $\mathbf{g}^t = \nabla f(\theta^t) + \Delta^t$, the above gives us

$$f(\theta^{t+1}) \leq f(\theta^t) - \eta \cdot \langle \nabla f(\theta^t), \mathbf{g}^t \rangle + \frac{H\eta^2}{2} \|\mathbf{g}^t\|_2^2$$

$$\begin{aligned}
&= f(\boldsymbol{\theta}^t) - \eta \cdot \langle \nabla f(\boldsymbol{\theta}^t), \nabla f(\boldsymbol{\theta}^t) + \boldsymbol{\Delta}^t \rangle + \frac{H\eta^2}{2} \left(\|\nabla f(\boldsymbol{\theta}^t) + \boldsymbol{\Delta}^t\|_2^2 \right) \\
&= f(\boldsymbol{\theta}^t) - \eta \cdot \|\nabla f(\boldsymbol{\theta}^t)\|_2^2 - \eta \cdot \langle \nabla f(\boldsymbol{\theta}^t), \boldsymbol{\Delta}^t \rangle + \frac{H\eta^2}{2} \left(\|\nabla f(\boldsymbol{\theta}^t) + \boldsymbol{\Delta}^t\|_2^2 \right)
\end{aligned}$$

Now, the Cauchy-Schwartz inequality along with the bound on the bias gives us $-\eta \cdot \langle \nabla f(\boldsymbol{\theta}^t), \boldsymbol{\Delta}^t \rangle \leq \eta\delta \cdot \|\nabla f(\boldsymbol{\theta}^t)\|_2^2$ as well as $\|\nabla f(\boldsymbol{\theta}^t) + \boldsymbol{\Delta}^t\|_2^2 \leq 2(1 + \delta^2) \cdot \|\nabla f(\boldsymbol{\theta}^t)\|_2^2$. Using these gives us

$$\begin{aligned}
f(\boldsymbol{\theta}^{t+1}) &\leq f(\boldsymbol{\theta}^t) - \eta(1 - \delta - \eta H(1 + \delta^2)) \cdot \|\nabla f(\boldsymbol{\theta}^t)\|_2^2 \\
&\leq f(\boldsymbol{\theta}^t) - \frac{\eta(1 - \delta)}{2} \cdot \|\nabla f(\boldsymbol{\theta}^t)\|_2^2,
\end{aligned}$$

since we chose $\eta \leq \frac{(1-\delta)}{2H(1+\delta^2)}$. Reorganizing, taking a telescopic sum over all t , using $f(\boldsymbol{\theta}^{T+1}) \geq f(\boldsymbol{\theta}^*)$ and making an averaging argument tells us that since we set, for any $T > 0$, it must be the case that for some $t \leq T$, we have

$$\|\nabla f(\boldsymbol{\theta}^t)\|_2^2 \leq \frac{2(f(\boldsymbol{\theta}^0) - f(\boldsymbol{\theta}^*))}{\eta(1 - \delta)T}$$

This proves the first part. For the second part, we yet again invoke smoothness to get

$$f(\boldsymbol{\theta}^{t+1}) \leq f(\boldsymbol{\theta}^t) + \langle \nabla f(\boldsymbol{\theta}^t), \boldsymbol{\theta}^{t+1} - \boldsymbol{\theta}^t \rangle + \frac{H}{2} \|\boldsymbol{\theta}^{t+1} - \boldsymbol{\theta}^t\|_2^2$$

Since we used the update $\boldsymbol{\theta}^{t+1} = \boldsymbol{\theta}^t - \eta \cdot \mathbf{g}^t$, the above gives us

$$\begin{aligned}
f(\boldsymbol{\theta}^{t+1}) &\leq f(\boldsymbol{\theta}^t) - \eta \cdot \langle \nabla f(\boldsymbol{\theta}^t), \mathbf{g}^t \rangle + \frac{H\eta^2}{2} \|\mathbf{g}^t\|_2^2 \\
&= f(\boldsymbol{\theta}^t) - \eta \cdot \langle \nabla f(\boldsymbol{\theta}^t), \mathbf{g}^t \rangle + \frac{H\eta^2}{2} \left(\|\nabla f(\boldsymbol{\theta}^t) + \boldsymbol{\Delta}^t\|_2^2 + \|\mathbf{g}^t - \nabla f(\boldsymbol{\theta}^t) - \boldsymbol{\Delta}^t\|_2^2 \right) \\
&\quad - H\eta^2 \langle \nabla f(\boldsymbol{\theta}^t) + \boldsymbol{\Delta}^t, \mathbf{g}^t - \nabla f(\boldsymbol{\theta}^t) - \boldsymbol{\Delta}^t \rangle
\end{aligned}$$

Taking conditional expectations on both sides gives us

$$\mathbb{E} [f(\boldsymbol{\theta}^{t+1})] \leq f(\boldsymbol{\theta}^t) - \eta \cdot \|\nabla f(\boldsymbol{\theta}^t)\|_2^2 - \eta \cdot \langle \nabla f(\boldsymbol{\theta}^t), \boldsymbol{\Delta}^t \rangle + \frac{H\eta^2}{2} \left(\|\nabla f(\boldsymbol{\theta}^t) + \boldsymbol{\Delta}^t\|_2^2 + \sigma^2 \right)$$

Now, the Cauchy-Schwartz inequality along with the bound on the bias gives us $-\eta \cdot \langle \nabla f(\boldsymbol{\theta}^t), \boldsymbol{\Delta}^t \rangle \leq \eta\delta \cdot \|\nabla f(\boldsymbol{\theta}^t)\|_2^2$ as well as $\|\nabla f(\boldsymbol{\theta}^t) + \boldsymbol{\Delta}^t\|_2^2 \leq 2(1 + \delta^2) \cdot \|\nabla f(\boldsymbol{\theta}^t)\|_2^2$. Using these and applying a total expectation gives us

$$\begin{aligned}
\mathbb{E} [f(\boldsymbol{\theta}^{t+1})] &\leq \mathbb{E} [f(\boldsymbol{\theta}^t)] - \eta(1 - \delta - \eta H(1 + \delta^2)) \cdot \mathbb{E} [\|\nabla f(\boldsymbol{\theta}^t)\|_2^2] + \frac{H\eta^2}{2} \cdot \sigma^2 \\
&\leq \mathbb{E} [f(\boldsymbol{\theta}^t)] - \frac{\eta(1 - \delta)}{2} \cdot \mathbb{E} [\|\nabla f(\boldsymbol{\theta}^t)\|_2^2] + \frac{H\eta^2}{2} \cdot \sigma^2
\end{aligned}$$

where the second step follows since we set $\eta \leq \frac{(1-\delta)}{2H(1+\delta^2)}$. Reorganizing, taking a telescopic sum over all t , using $f(\boldsymbol{\theta}^{T+1}) \geq f(\boldsymbol{\theta}^*)$ and making an averaging argument tells us that for any $T > 0$, it must be the case that for some $t \leq T$, we have

$$\mathbb{E} [\|\nabla f(\boldsymbol{\theta}^t)\|_2^2] \leq \frac{2(f(\boldsymbol{\theta}^0) - f(\boldsymbol{\theta}^*))}{\eta(1 - \delta)T} + \frac{H\eta\sigma^2}{1 - \delta}$$

However, since we also took care to set $\eta = \frac{1}{C\sqrt{T}}$, we get

$$\mathbb{E} [\|\nabla f(\boldsymbol{\theta}^t)\|_2^2] \leq \frac{2C(f(\boldsymbol{\theta}^0) - f(\boldsymbol{\theta}^*)) + H\sigma^2/C}{(1 - \delta)\sqrt{T}}$$

which proves the second part and finishes the proof. \square